Scientific Report No. 90

A TWO-PORT RECTANGULAR MICROSTRIP ANTENNA ELEMENT

by

Anders G. Derneryd

July 1987

Electromagnetics Laboratory
Department of Electrical and Computer Engineering
University of Colorado
Boulder, CO 80309

On leave from

Ericsson Radio Systems AB
S-43126 Molndal, Sweden

ABSTRACT

The transmission-line model is used to design and analyze a two-port rectangular microstrip antenna element. The input and the output ports are located along the non-radiating sides. The antenna input port is matched and the radiated power controlled by properly selecting the locations of these ports. The width of the patch is adjusted in order to ensure a phase reversal of the two radiating slot voltages to give a broadside beam.

Two different spacings of the ports are possible. One configuration is when the input and output ports are placed close to each other on the same side of the centerline of the patch. In the other design the ports are connected to the patch on opposite sides of the centerline. The phase difference of the transmitted signal for the two possible cases is about 180 degrees.

The resonant lengths of the two-port element are slightly different for the two possible output port locations. This is equivalent to a shift in the resonant frequency when the port is moved from one side of the centerline to the opposite side.

The two-port microstrip antenna element has a much broader standing wave ratio bandwidth, up to 20 %, than the single-fed element. Thus, the two-port patch is a suitable candidate as a radiating element in a series-fed linear array.

CONTENTS

		Page
1.	INTRODUCTION	4
2.	TWO-PORT MICROSTRIP RESONATOR	6
3.	DESIGN EQUATIONS	10
4.	SIMULATIONS	20
4.1	Constant patch width	20
4.2	Optimum patch width	27
5.	BANDWIDTH CHARACTERISTICS	34
5.1	Preliminaries	34
5.2	Constant patch width	36
5.3	Optimum patch width	39
6.	CONCLUSIONS	45
	REFERENCES	47
	APPENDIX	48

1. INTRODUCTION

The simplest form of feed system for linear microstrip array antennas is the series feeding. The resonant elements are interconnected with a narrow, high impedance microstrip transmission line. The spacing between the radiating elements is chosen to produce the required phase distribution across the aperture. In order to taper the amplitude distribution, the widths of rectangular patches are changed down the array.

Two types of series-fed microstrip arrays are feasible. The resonant or standing-wave antenna where the microstrip line is terminated in an open or short circuit and the non-resonant or traveling-wave antenna where the end of the microstrip line is terminated in a resistive match. The resonant array usually has a broadside pointing beam. End-fed and center-fed resonant linear arrays of half wavelength rectangular patches have been described [1,2]. Corporate-fed planar microstrip antennas incorporating end-fed resonant linear arrays have also been presented [3,4]. The useful bandwidth in this type of array is limited by the input impedance frequency variation.

The last resonator is matched to form a non-resonant array if an off-broadside beam or frequency scanning are required. An end-fed traveling-wave microstrip array with varying patch widths to control the radiation sidelobes has been published [2]. A limiting factor in this type of array is the main beam direction changes with

frequency. The bandwidth is limited by the maximum allowed beam squint or increased sidelobe level.

In a frequency scanning array the beam scan can be enhanced by increased line lengths between the microstrip radiating elements [5,6]. The coupling to the elements is performed by quarter wavelength transformers at the input and output ports along the radiating edges. The characteristic impedances of the transformers and of the patch resonators are determined from three conditions. Namely, the elements are matched at the input port at the center frequency. Secondly, the phase shift through the resonators is fixed to the same value for all elements in the array. Finally, how the input power is divided into radiated and transmitted power. A restriction in this kind of microstrip array is the minimum line width of the coupling transformers set by the photo lithographic technique.

This report describes a matched, two-port microstrip antenna element of rectangular shape with the input and output ports connected to the non-radiating edges. The ratio between the radiated and transmitted power is controlled by the location of these ports. The bandwidth of the microstrip patch is increased by loading it in this way. Such an antenna element is particularly suitable for series-fed array applications.

2. TWO-PORT MICROSTRIP RESONATOR

The microstrip resonator consists of a thin dielectric sheet of permittivity ε_r and thickness h on a ground-plane. There is a metallic patch of width w and length l on top of the dielectric. The fundamental mode of propagation is a quasi-TEM mode. The mode is quasi because the medium is inhomogeneous. It is therefore convenient to introduce an effective dielectric constant ε_e which takes the inhomogenity into account and it is used for finding the characteristic impedance [7].

$$\varepsilon_e = \frac{\varepsilon_r + 1}{2} + \frac{\varepsilon_r - 1}{2}\left(1 + 10\frac{h}{w}\right)^{-\frac{1}{2}} \tag{2.1}$$

$$Z_0 = \begin{cases} \dfrac{60}{\sqrt{\varepsilon_e}} \ln\left(\dfrac{8\,h}{w} + 0.25\,\dfrac{w}{h}\right) & \dfrac{w}{h} < 1 \\ \dfrac{120\,\pi}{\sqrt{\varepsilon_e}}\left[\dfrac{w}{h} + 1.393 + 0.667\ln\left(\dfrac{w}{h} + 1.444\right)\right]^{-1} & \dfrac{w}{h} > 1 \end{cases} \tag{2.2}$$

These formulas may be adjusted for the finite thickness of the metallic strips as well as for the dispersion effects due to the inhomogenity mentioned above. Since these corrections are small in most practical cases they have been neglected in the following sections.

The two-port microstrip antenna element, shown in Figure 2.1, is resonant when the length l is approximately half a wavelength in the dielectric. The voltage is then maximum at the edges terminated in open circuits. Along these sides the voltage is assumed to be constant and it is useful to treat each radiating edge as an independent slot.

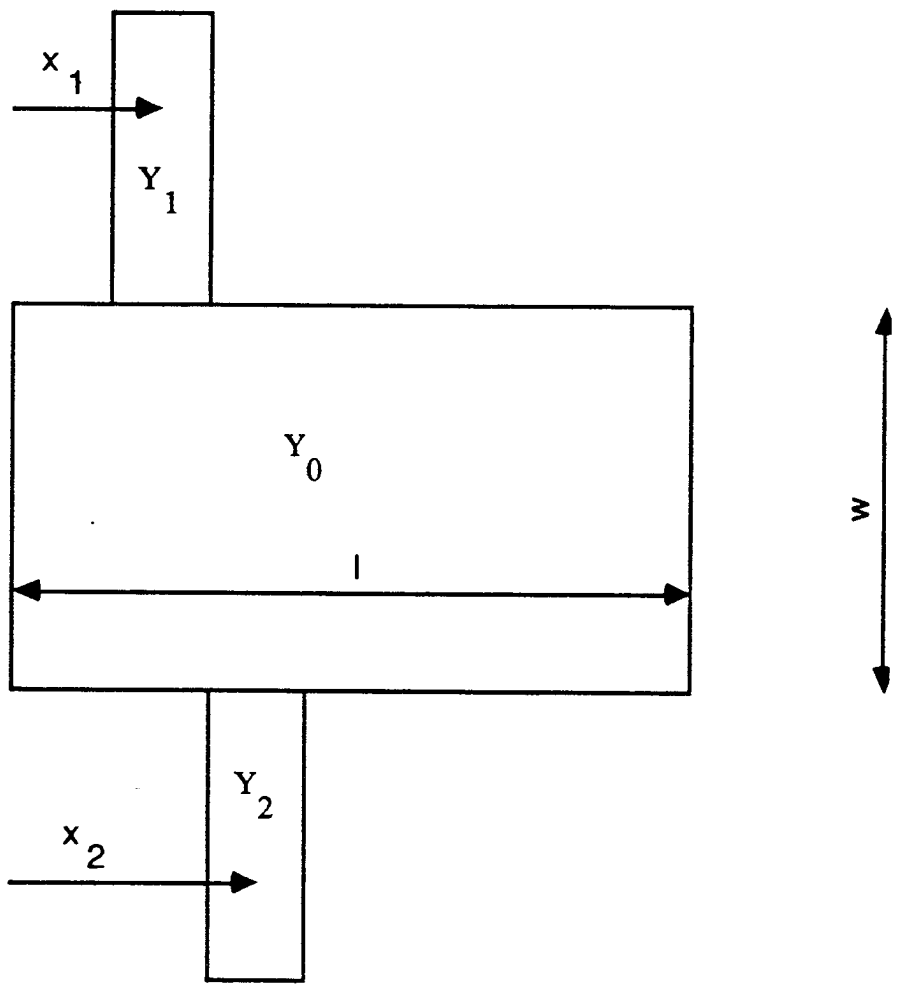

Figure 2.1 Two-port microstrip antenna element

The radiation conductance of a single slot is given by [8]

$$G = \begin{cases} \dfrac{w_e^2}{90\,\lambda_0^2} & \dfrac{w_e}{\lambda_0} < 0.35 \\ \dfrac{w_e}{120\,\lambda_0} - \dfrac{1}{60\,\pi^2} & 0.35 < \dfrac{w_e}{\lambda_0} < 2.0 \end{cases} \qquad (2.3)$$

where

$$w_e = \frac{120\,\pi\,h}{Z_0\sqrt{\varepsilon_e}} \qquad (2.4)$$

and λ_0 is the free-space wavelength. Power loss due to surface waves can easily be added into the above expressions. Also dielectric and ohmic losses can approximately be accounted for by introducing equivalent admittances in the network model.

The input and output ports, denoted with subscripts 1 and 2, respectively are located along the side edges, where the voltage varies approximately cosinusoidally. The fringing fields at these edges are accounted for by the introduction of an effective width w_e as given in eqn 2.4.

A transmission line model is used to design and analyze the two-port microstrip antenna element neglecting external interaction between the slots [9]. The slot susceptances have been replaced by equivalent

line extensions [1] to simplify the model shown in Figure 2.2. This is adequate from a network point of view as long as the extensions are small. However, care must be used when calculating external coupling or radiation patterns since the phase centers of the radiating slots have been shifted outwards.

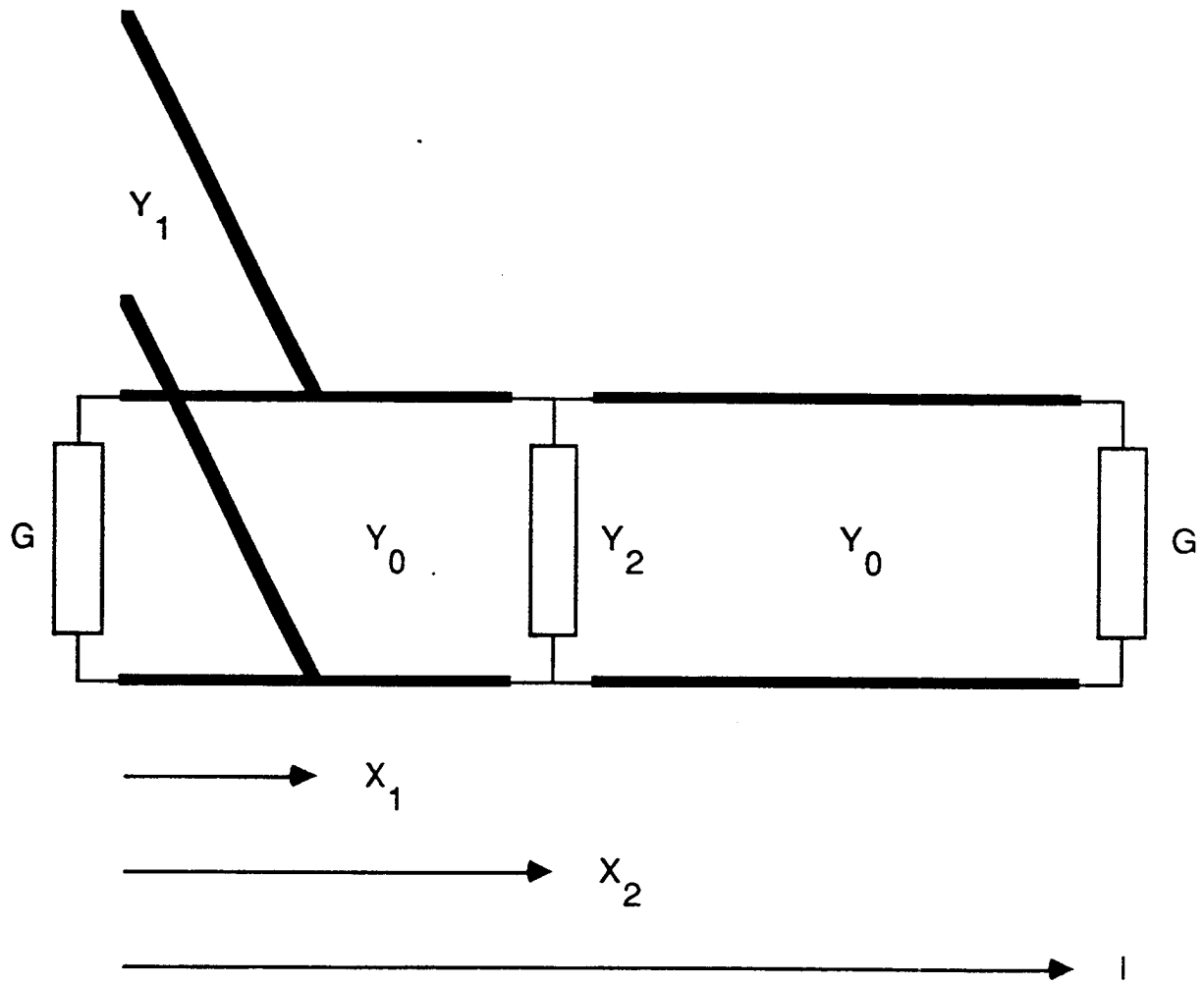

Figure 2.2 Transmission line model of a two-port microstrip antenna element.

The effects of higher order modes excited at the feed points can be taken into account by introducing series inductances in the network model. However, these have been omitted for the sake of clearness in the derivations to follow. The junction discontinuites add phase shifts proportional to the size of the discontinuity. A rigorous solution of the radiation properties using two-dimensional analysis is time consuming [9]. However, the basic properties can be found and understood from a simplified theory using the transmission-line model.

3. DESIGN EQUATIONS

The power T, transmitted through the antenna element from the input port to the output port, is controlled by the locations, x_1 and x_2 respectively, of these ports. Futhermore, the total power radiated, represented by R, is equal to the power lost in the equivalent slot admittances. Assuming no other losses, R and T add up to unity.

At the resonant frequency the input port is matched. This requirement is fulfilled if the following conditions are met.

$$\begin{cases} Y_1 = G_L + G_R \\ B_L = -B_R \end{cases} \tag{3.1}$$

where $Y_L = G_L + jB_L$ and $Y_R = G_R + jB_R$ are the admittances seen at the input port looking to the left and to the right, respectively.

The power radiated at the left slot is equal to the power dissipated in G_L since the input port is matched and assuming no other losses. Similarly, the sum of the power radiated at the right slot and the power transmitted to the output port is equal to the power dissipated in G_R. Thus,

$$\begin{cases} G_L = \frac{R}{2} Y_1 \\ G_R = \left(T + \frac{R}{2}\right) Y_1 \end{cases} \tag{3.2}$$

The admittance at the input port seen to the left is found by transforming the left slot conductance G a distance x_1 to the input port. This gives

$$Y_L = Y_0 \frac{Y_0 G\left(1 + \tan^2 \beta x_1\right) + j\left(Y_0^2 - G^2\right) \tan \beta x_1}{Y_0^2 + G^2 \tan^2 \beta x_1} \tag{3.3}$$

where β is the propagation constant in the dielectric underneath the patch assuming no losses. This expression is split into a real and an imaginary part. The real part is equal to G_L given in eqn 3.2. This yields an expression for the location of the input port in terms of radiated power ratio, slot conductance and characteristic line impedances.

$$\tan^2 \beta x_1 = \frac{Y_0^2}{G} \frac{\frac{R}{2} Y_1 - G}{Y_0^2 - \frac{R}{2} Y_1 G} \tag{3.4}$$

A minimum value of the radiated power ratio is set by practical values of the parameters as follows

$$R > 2 \frac{G}{Y_1} \tag{3.5}$$

Thus, a certain portion of the input power is always radiated for a fixed patch width. However, this fraction can be made as small as required by decreasing the radiation slot conductance given in eqn 2.3 and hence the width of the patch.

At the resonant frequency the susceptances at the input port seen to the left and to the right are expressed using eqns 3.3 and 3.4. Thus, the input admittances become

$$\begin{cases} G_L = \frac{R}{2} Y_1 \\ B_L = \frac{Y_0^2 - \frac{R}{2} Y_1 G}{Y_0} \tan \beta x_1 \end{cases} \tag{3.6}$$

and

$$\begin{cases} G_R = \left(1 - \dfrac{R}{2}\right) Y_1 \\ B_R = \dfrac{\dfrac{R}{2} Y_1 G - Y_0^2}{Y_0} \tan \beta x_1 \end{cases} \tag{3.7}$$

The next step is to find the location of the output port and the resonant length of the patch. This is done by transforming the right slot conductance and the right input admittance to the same point, namely the location of the output port. The difference between these so obtained expressions is equal to the characteristic admittance Y_2 of the output line. This condition gives two equations, one for the real part and one for the imaginary part.

$$\frac{Y_0^2 G_R}{G_R^2 \sin^2 \beta (x_1 - x_2) + \left[B_R \sin \beta (x_1 - x_2) - Y_0 \cos \beta (x_1 - x_2)\right]^2} =$$

$$= Y_2 + \frac{Y_0^2 G}{Y_0^2 \cos^2 \beta (1 - x_2) + G^2 \sin^2 \beta (1 - x_2)} \tag{3.8}$$

$$\frac{Y_0 B_R \left[\cos^2\beta(x_1 - x_2) - \sin^2\beta(x_1 - x_2)\right] + \left(Y_0^2 - G_R^2 - B_R^2\right) \sin\beta(x_1 - x_2) \cos\beta(x_1 - x_2)}{G_R^2 \sin^2 \beta (x_1 - x_2) + \left[B_R \sin \beta (x_1 - x_2) - Y_0 \cos \beta (x_1 - x_2)\right]^2} =$$

$$= \frac{\left(Y_0^2 - G^2\right) \sin \beta (1 - x_2) \cos \beta (1 - x_2)}{Y_0^2 \cos^2 \beta (1 - x_2) + G^2 \sin^2 \beta (1 - x_2)}$$

The left hand sides of these expressions are functions of the distance between the input and output ports, while the right hand sides are

functions of the distance from the output port to the right slot. Thus, for a fixed patch size eqn 3.8 is a set of two coupled non-linear equations with two real unknowns, (x_1-x_2) and $(l-x_2)$. It is solved with numerical techniques using a finite difference approximation of the Jacobian [10].

Generally, there are many solutions to this problem since it is always possible to add multiples of the wavelength to the solutions obtained. However, for a resonant length close to half a wavelength there are two distinctive solutions. One solution is when the input and output ports are located close to each other on the same side of the centerline of the patch. In the other solution, the output port is shifted to the other side of the centerline closer to the right slot than to the left slot.

A physical insight to the above problem is gained by using the Smith-chart to find the location of the output port as well as the resonant length of the patch. An example is presented in Figure 3.1. The characteristic impedances of the input and output lines are 50 ohm. The radiation resistance is assumed to be 1000 ohm at each slot and the characteristic impedance of the patch is 20 ohm.

The location of the input port is 45 degrees (0.125 wavelengths) from the radiating edge as given by eqn 3.4 when the total power radiated is set to 20% of the input power. The equivalent admittances seen at the input port are thus completely determined and they are given by eqns 3.6 and 3.7. The left normalized input admittance is

$y_L = 0.0400 + j0.9996$ and the right normalized input admittance is $y_R = 0.3600 - j0.9996$. The latter value is plotted in the Smith-chart in Figure 3.1. Now y_R is transformed to a point where the sum of the transformed admittance and the normalized output characteristic admittance is equal to the right slot conductance transformed to the same point. Two solutions are possible as seen in the Smith-chart. One solution gives a distance of 5 degrees (0.014 wavelengths) between the input and output ports. The second solution gives a distance of 81 degrees (0.226 wavelengths). Finally, the distances between the output port and the right slot location are 130 degrees (0.362 wavelengths) and 50 degrees (0.138 wavelengths), respectively. Thus the resonant lengths are 180 degrees (0.501 wavelengths) and 176 degrees (0.489 wavelengths), respectively. The network models of these two basic solutions are given in Figure 3.2.

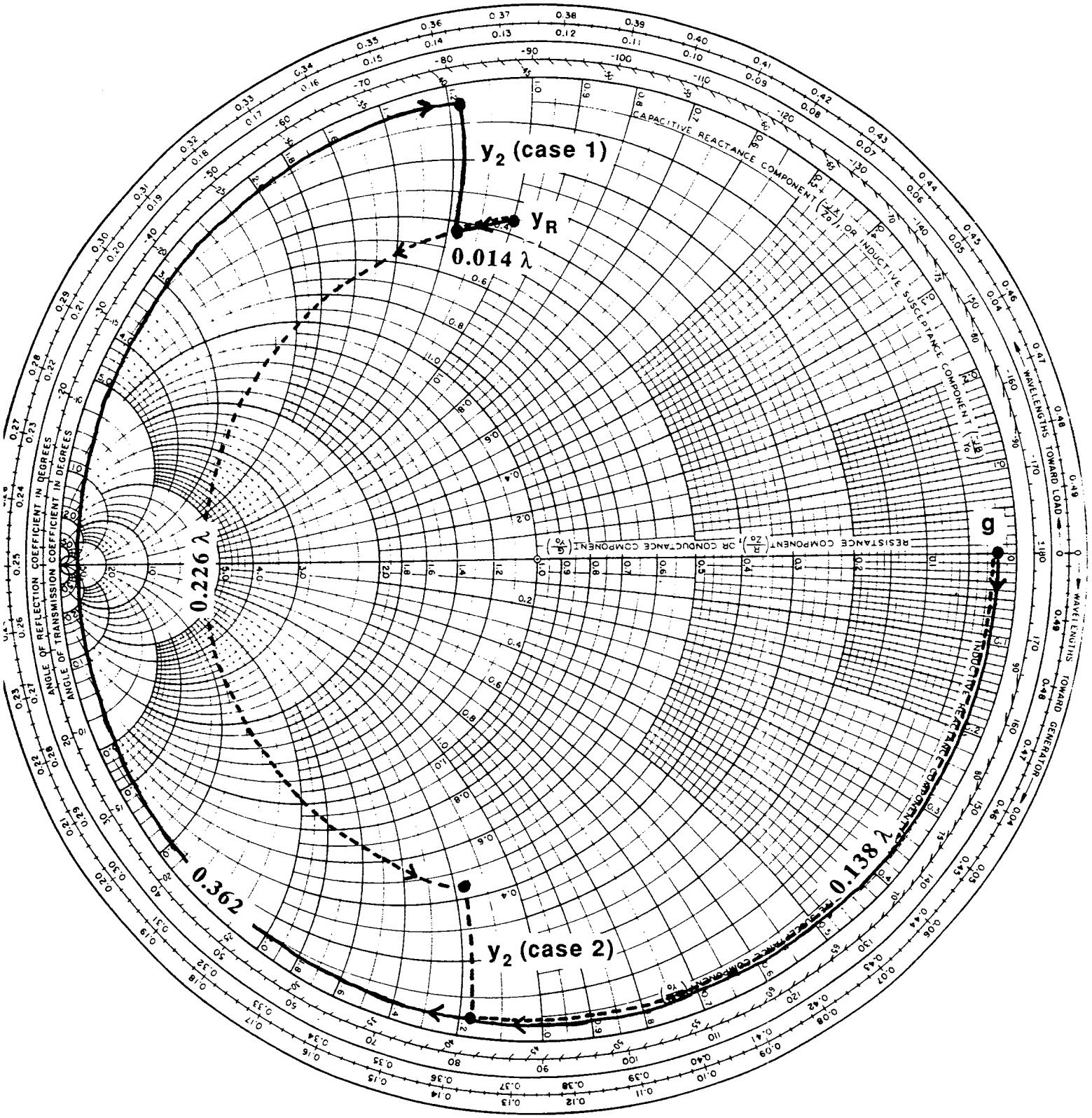

Figure 3.1 Smith-chart representation to find the location of the output port and the resonant length of the patch

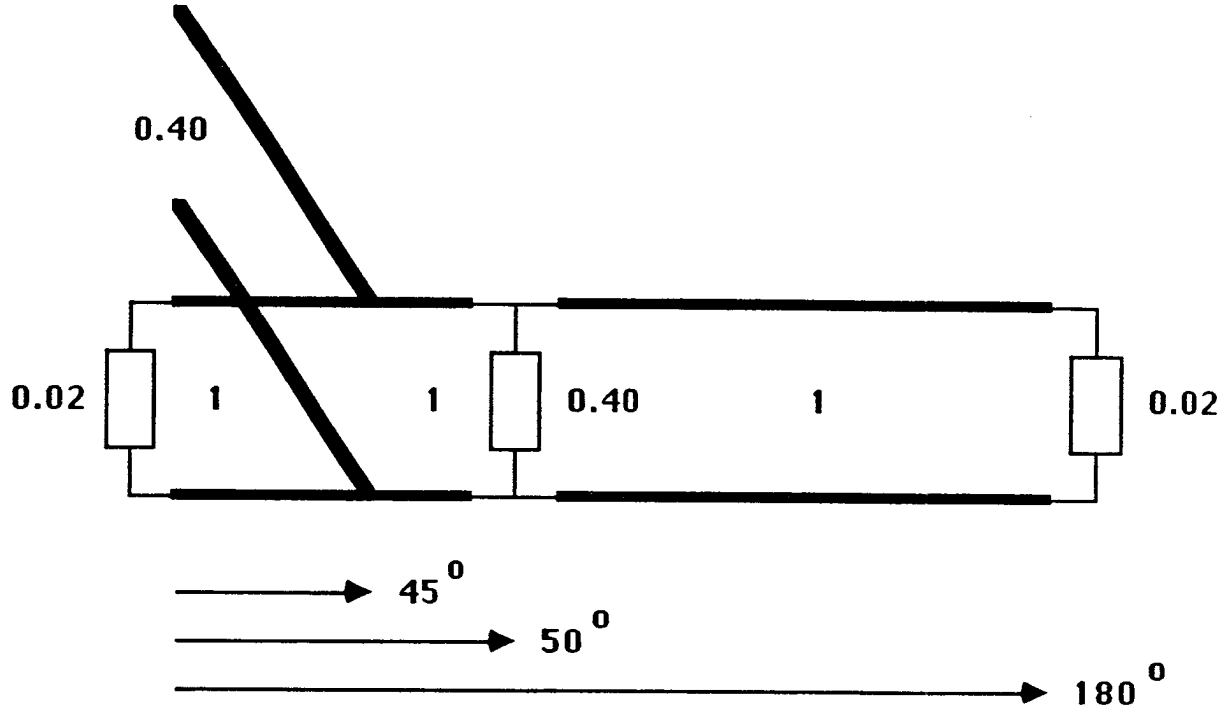

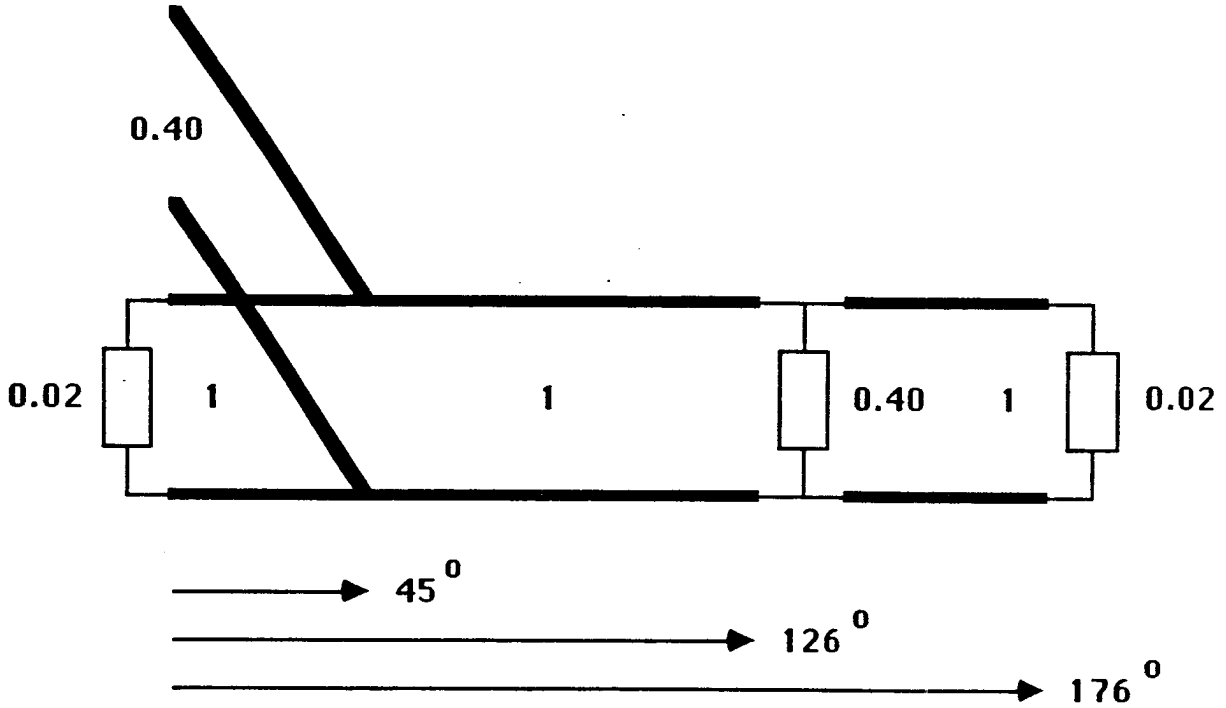

Figure 3.2 Network models of two possible solutions to the problem solved in Figure 3.1

The locations of the input and output ports according to eqn 3.8 do not imply a 180 degrees phase shift between the slot voltages in Figure 3.2. However, this is a necessary requirement if a broadside beam is desirable. Thus, a third equation is introduced that relates the phases of the radiating slot voltages. The voltages V_{SL} and V_{SR} across the left and rigth slot conductances, respectively are for a matched two-port element given by

$$\begin{cases} V_{SL} = \left(\cos \beta x_1 - j \dfrac{Y_L}{Y_0} \sin \beta x_1 \right) V_1^+ \\ V_{SR} = [\dfrac{Y_2}{Y_0} \sin \beta(1 - x_2) \left\{ \dfrac{Y_R}{Y_0} \sin \beta(x_2 - x_1) + j \cos \beta(x_2 - x_1) \right\} + \\ \quad + \cos \beta(1 - x_1) - j \dfrac{Y_R}{Y_0} \sin \beta(1 - x_1)] V_1^+ \end{cases} \tag{3.9}$$

where V_1^+ is the incoming voltage at the input port.

The third equation is thus

$$\arctan \frac{\frac{Y_2}{Y_0}\sin\beta\left(1-x_2\right)\left[\frac{B_R}{Y_0}\sin\beta\left(x_2-x_1\right)+\cos\beta\left(x_2-x_1\right)\right]-\frac{G_R}{Y_0}\sin\beta\left(1-x_1\right)}{\frac{Y_2 G_R}{Y_0^2}\sin\beta\left(1-x_2\right)\sin\beta\left(x_2-x_1\right)+\cos\beta\left(1-x_1\right)+\frac{B_R}{Y_0}\sin\beta\left(1-x_1\right)} -$$

$$- \arctan \frac{-\frac{G_L}{Y_0}\sin\beta x_1}{\cos\beta x_1+\frac{B_L}{Y_0}\sin\beta x_1} = \pi \tag{3.10}$$

The parameter to solve for is the width of the patch. The admittances in expressions 3.8 and 3.10 can all be expressed in terms of the width w for a particular substrate and fixed input and output impedance levels. With this added restriction on the slot phases it is not always possible to find two basically different locations of the ports.

The solution for the one-port microstrip antenna element is achieved as a special case when $Y_2 = 0$. Thus all power is radiated and R equals one in eqn 3.4. The location of the input port for a matched one-port rectangular patch antenna is

$$\cos 2\beta x_1 = \frac{4 Y_0^2 G - Y_1\left(Y_0^2+G^2\right)}{Y_1\left(Y_0^2-G^2\right)} \tag{3.11}$$

This expression is for practical values of the parameters ($G << Y_0$) rewritten as

$$\cos^2 \beta x_1 = \frac{2G}{Y_1} \tag{3.12}$$

The resonant length is always half a wavelength since the end susceptances are replaced with equivalent line extensions to account for the fringing fields.

4. SIMULATIONS

4.1 Constant patch width

The locations of the input and output ports as well as the resonant length of a constant-width rectangular patch is calculated as a function of the power transmission ratio. The results are plotted in Figure 4.1 for the case described in the previous section and graphically solved in Figure 3.1. The input and output line impedances are 50 ohm, the microstrip patch impedance is 20 ohm and the slot radiation resistances are 1000 ohm each. Two cases are shown in the figure. Case 1 is the solution with the two ports relatively close to eath other, while the second case refers to a patch with ports on opposite sides of the centerline. The results for a 80% power transmission ratio agree very well with the solutions in Figure 3.2 which were obtained using the Smith-chart.

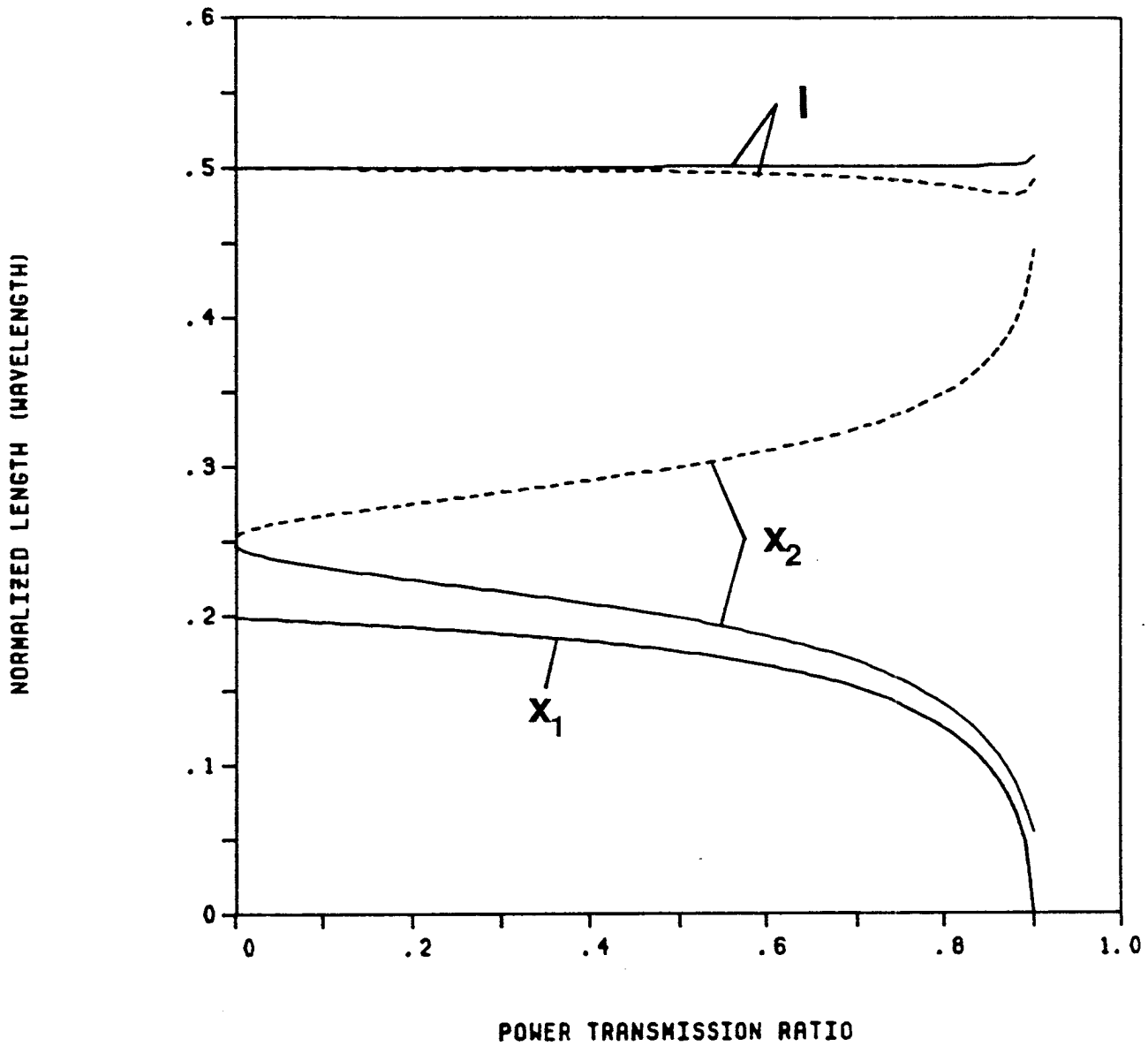

Figure 4.1 Computed port locations and resonant lengths of a rectangular patch as a function of the power transmission ratio. Z_0 = 20 ohm, Z_1 = 50 ohm, Z_2 = 50 ohm and G = 1 mS. —— = case 1, - - - = case 2

It is observed that the power transmission ratio is limited to 90%. This value is also obtainable from eqn 3.5 for the particular choice of parameters. The maximum power transmission ratio is achieved with the input port located at one of the radiating edges. Moving the input port towards the center of the patch, away from the radiating edge, increases the power radiated. The maximum radiated power is achieved with the output port close to the center of the patch where a voltage minimum occurs, thus minimizing the transmitted power. The distance between the input port and the output port decreases for case 1 as the power transmission ratio increases. The opposite is true in case 2 since the output port always moves towards the closest radiating slot with increasing power transmission ratio.

The resonant length of the patch is close to half a wavelength. However, it is slightly shorter in case 2 compared to case 1. A particular power transmission ratio can be obtained with different sets of parameters. For example by moving the feed point towards the radiating edge and at the same time increasing the input line impedance level or the slot conductance keeps the ratio unchanged.

The phases of the slot voltages and the output voltage are plotted in Figure 4.2 as a function of the power transmission ratio. The input voltage is used as a reference. The phases of the voltages are nearly constant in case 1 except for very small and very high power transmission ratios. In case 2 the phase of the right slot voltage changes 20 degrees over the possible range of power transmission ratios. Thus, it is not possible to obtain a 180 degree phase difference

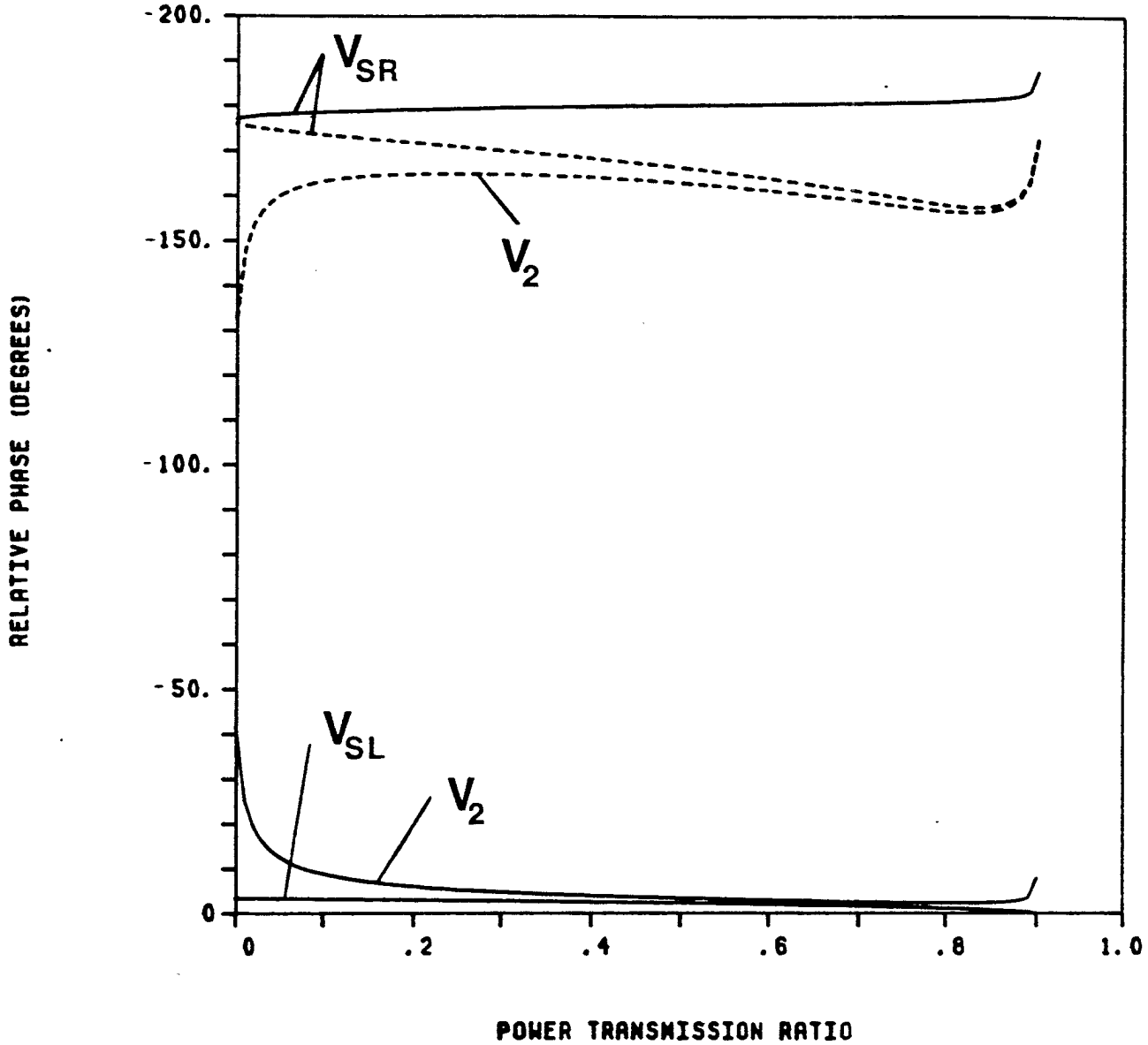

Figure 4.2 Computed phases as a function of the power transmission ratio for a rectangular patch. Z_0 = 20 ohm, Z_1 = 50 ohm, Z_2 = 50 ohm and G = 1 mS. —— = case 1, - - - = case 2

between the radiating slot voltages in case 2 without changing the width or the length of the patch. The phase of the output signal is shifted nearly 180 degrees as the location of the output port is switched from one side to the other side of the centerline.

The magnitude and the phase of the standing wave underneath the patch is shown in Figures 4.3 and 4.4, respectively for a 80% power transmission ratio. The input voltage at x_1 is used as a reference with unit magnitude and zero degree phase. Curves for two different locations of the output port are presented. It is observed in Figure 4.4 that the phase difference between the radiating slot voltages is not exactly 180 degrees in either case. There is a larger difference in case 2 compared to case 1. The standing wave pattern resembles a sinusoidal curve with a rapid phase change close to the center of the patch. However, there is a change in phase slope where the output port is located.

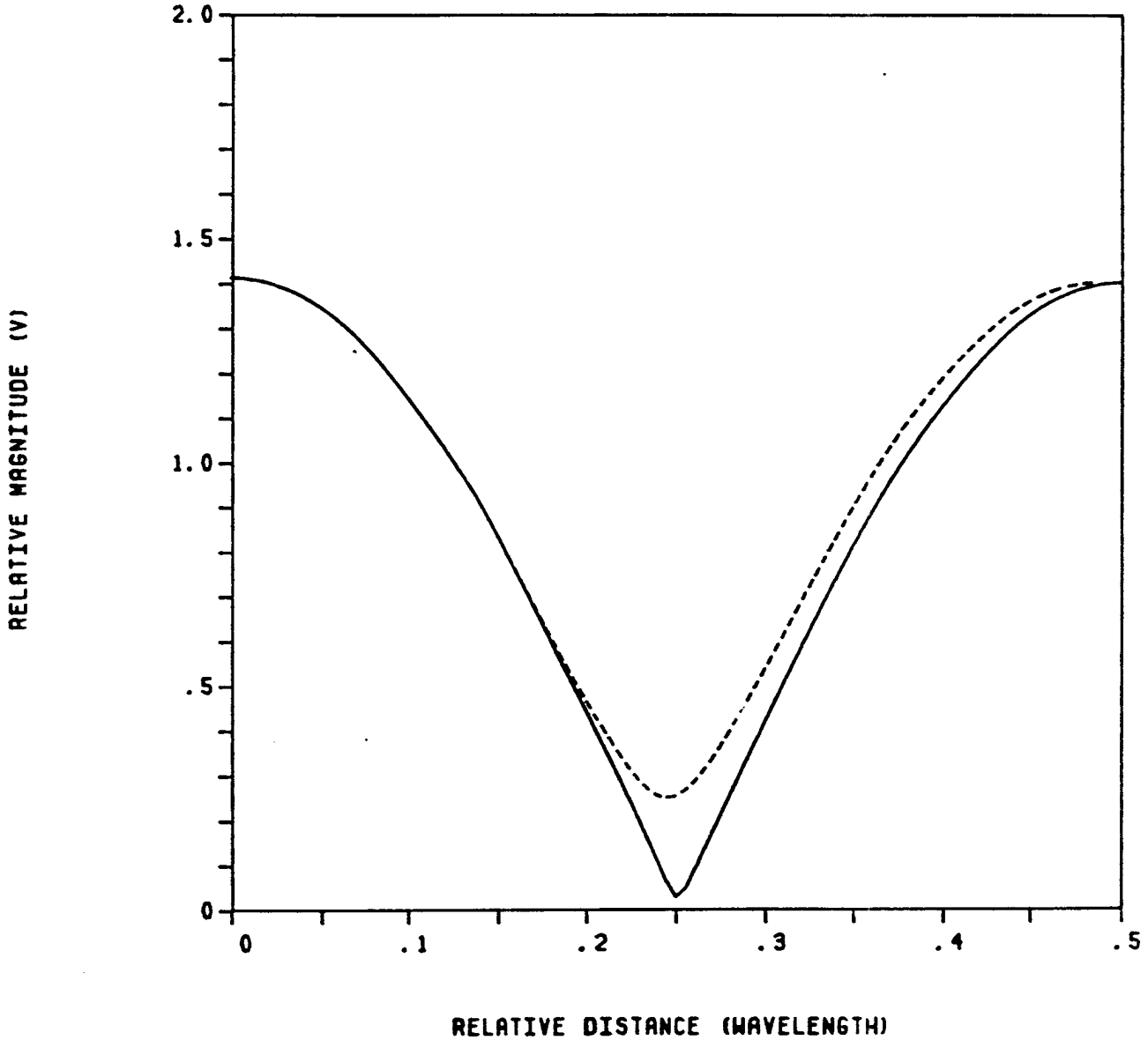

Figure 4.3 Relative magnitude of the standing wave underneath a rectangular patch. Z_0 = 20 ohm, Z_1 = 50 ohm, Z_2 = 50 ohm, G = 1 mS and T = 80%. —— = case 1, - - - = case2

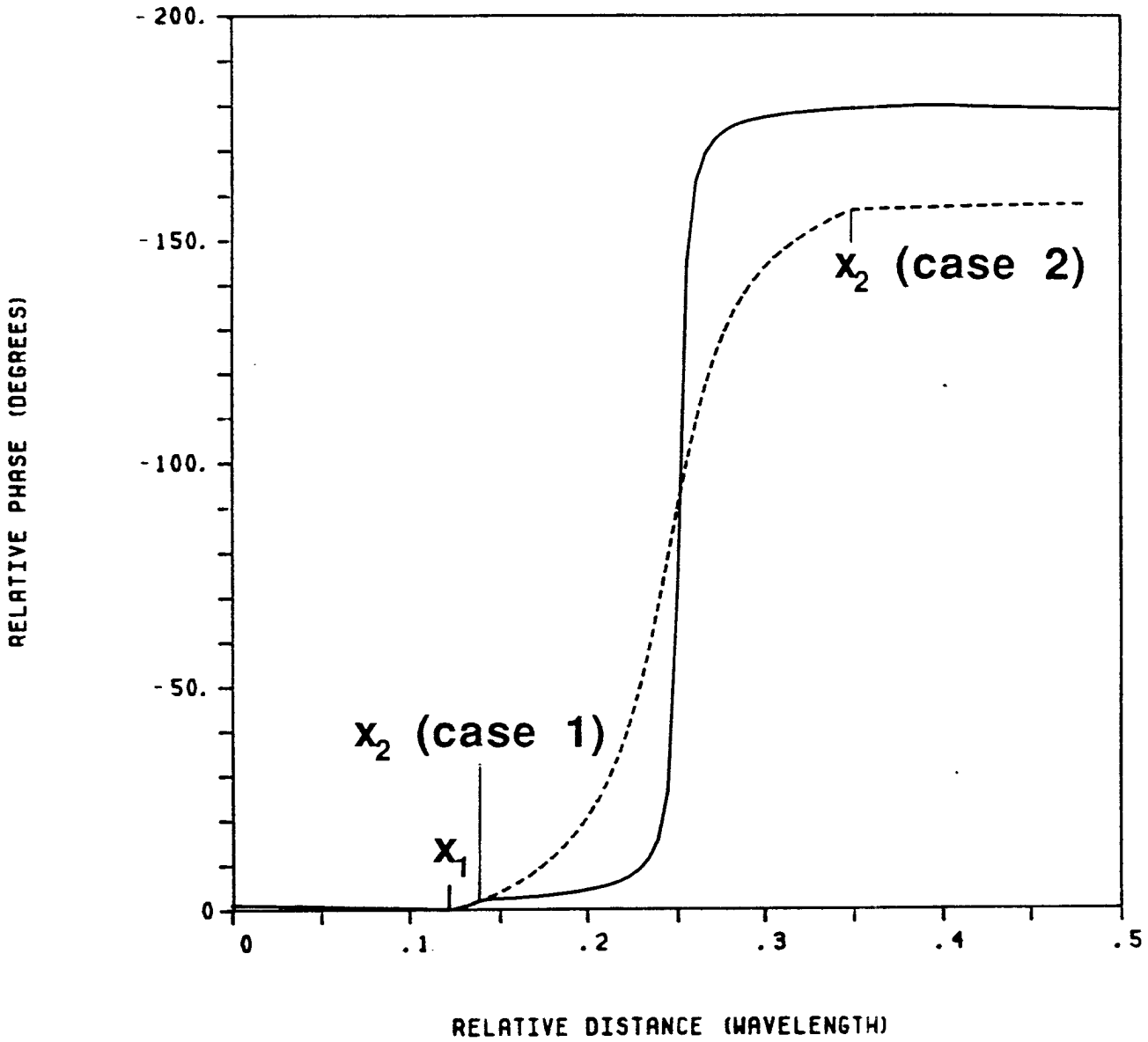

Figure 4.4 Relative phase of the standing wave underneath a rectangular patch. Z_0 = 20 ohm, Z_1 = 50 ohm, Z_2 = 50 ohm, G = 1 mS and T = 80%. —— = case 1, - - - = case2

4.2 Optimum patch width

As discussed in the previous section the phase difference between the radiating edges is not excatly 180 degrees. However, this can be accomplished by adjusting the width of the radiating patch. In the following paragraphs computer simulations have been performed for a particular choice of substrate parameters. The dielectric constant is 2.2 and the the thickness is either 1/32 in (0.794 mm) or 1/64 in (0.397 mm). The center frequency is 7.5 GHz. The variables to optimize are the location of the input and output ports, the resonant length of the patch and the width of the patch. The characteristic impedance levels of the input and output lines are held constant, 50 ohm or 75 ohm.

The first curve that is plotted is the location of the input and output ports as well as the resonant length as a function of the power transmission ratio. The results for two different substrate thicknesses are shown in Figure 4.5. It is hardly no difference between the two sets of curves. The same conclusion holds if the input and output impedance levels are increased to 75 ohm. The resonant length is close to half a wavelength in both cases. However, the physical length of the thicker patch is slightly longer than the thinner one, due to a smaller effective dielectric constant.

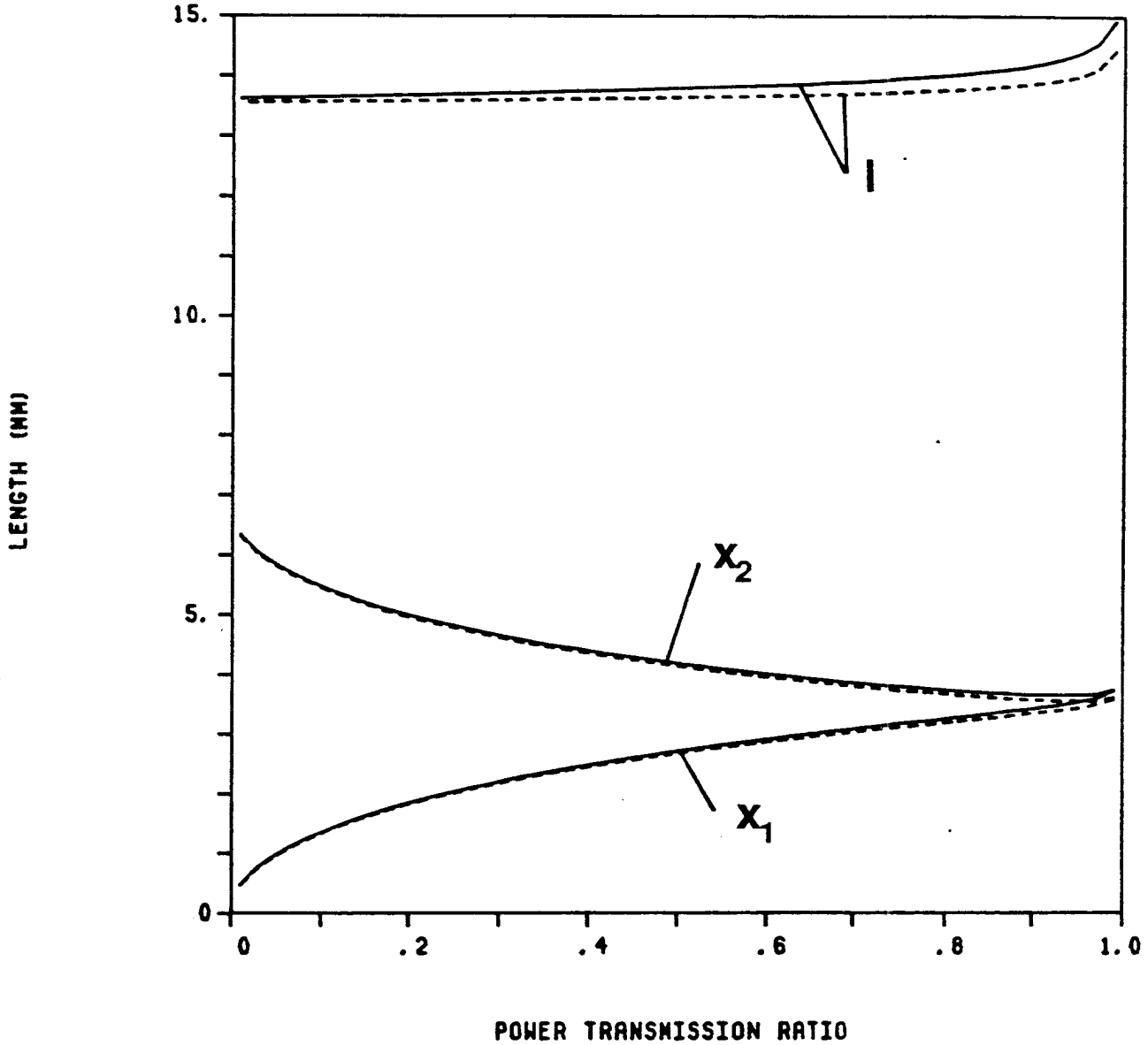

Figure 4.5 Locations of the input and output ports and the resonant length as a function of the power transmission ratio for a rectangular patch. Z_1 = 50 ohm, Z_2 = 50 ohm, f = 7.5 GHz and ε_r = 2.2. —— h = 1/32 in, - - - - h = 1/64 in.

The location of the input port moves toward the center of the patch as the power transmission ratio is increased. At the same time the spacing between the input and output ports decreases. For the case when no power is transmitted, the output port is located at the voltage minimum close to the center of the patch. Maximum power is transmitted when the input and output ports are located right across each other along the non-radiating edges.

The power transmission coefficient can approximately be expressed as a function of the input and output locations as [11]

$$T = \left| \frac{\cos \beta x_2}{\cos \beta x_1} \right|^2 \tag{4.1}$$

The width of the radiating patch as a function of the power transmission ratio is shown in Figure 4.6. The optimum width decreases with increased power transmission ratio. Thus, a narrow patch radiates less power than a wide one. All values of power transmission ratios are realizable which are not the case when the width is held constant. More power is radiated for the same patch width when the impedance levels of the input and output lines are increased.

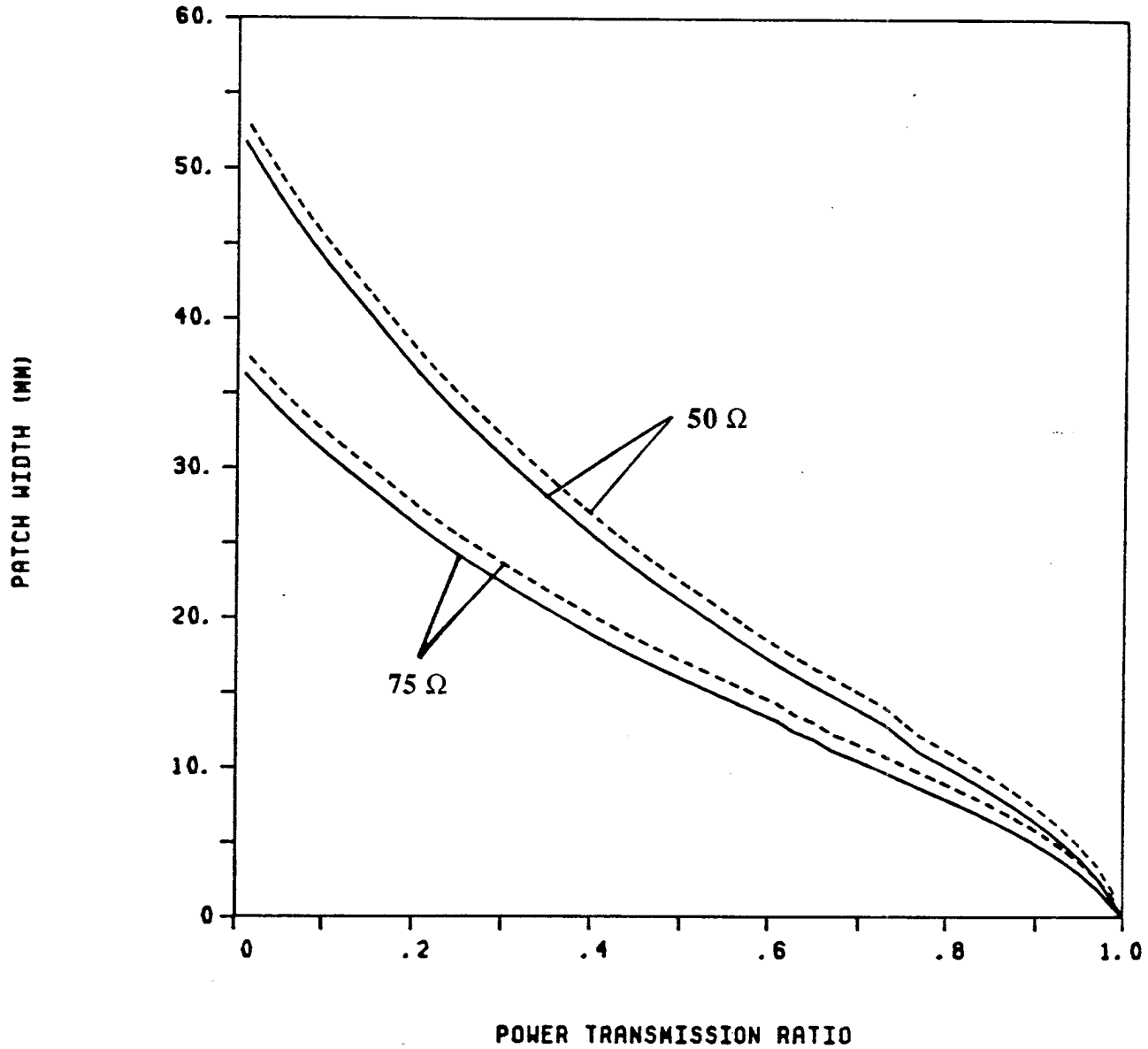

Figure 4.6 Optimum width of a rectangular patch as a function of the power transmission ratio. f = 7.5 GHz and $\varepsilon_r = 2.2$. —— h = 1/32 in, - - - - h=1/64 in

The slot conductance as a function of the patch width is plotted in Figure 4.7 for two different substrate thicknesses. The slot conductance increases linearly for patch widths larger than 13 mm. For smaller values it is a quadratic behavour as given in eqn 2.3. The steps in the curves are due to that the used slot admittance model is not continuous as a function of the patch width.

Although the phase difference between the radiating slot voltages is 180 degrees there is a very small change in the slot voltages relative to the input port voltage as the power transmission ratio is varied. In the cases studied it is less than 1 degree. However, the phase of the transmitted signal varies more. The output voltage for the matched two-port element is

$$V_2 = \left[\cos\beta\left(x_2 - x_1\right) - j\frac{Y_R}{Y_0}\sin\beta\left(x_2 - x_1\right) \right] V_1^+ \qquad (4.2)$$

The phase of the transmitted signal relative to the input signal is plotted in Figure 4.8 as a function the power transmission ratio. As shown the phase shift decreases as the loading increases. Changing the impedance level of the input and output lines has a minor effect on the output phase. However, the patch width is altered as the ratio and the impedence level are changed as shown in Figure 4.6. Increasing the thickness of the substrate will slightly increase the relative phase of the transmitted signal.

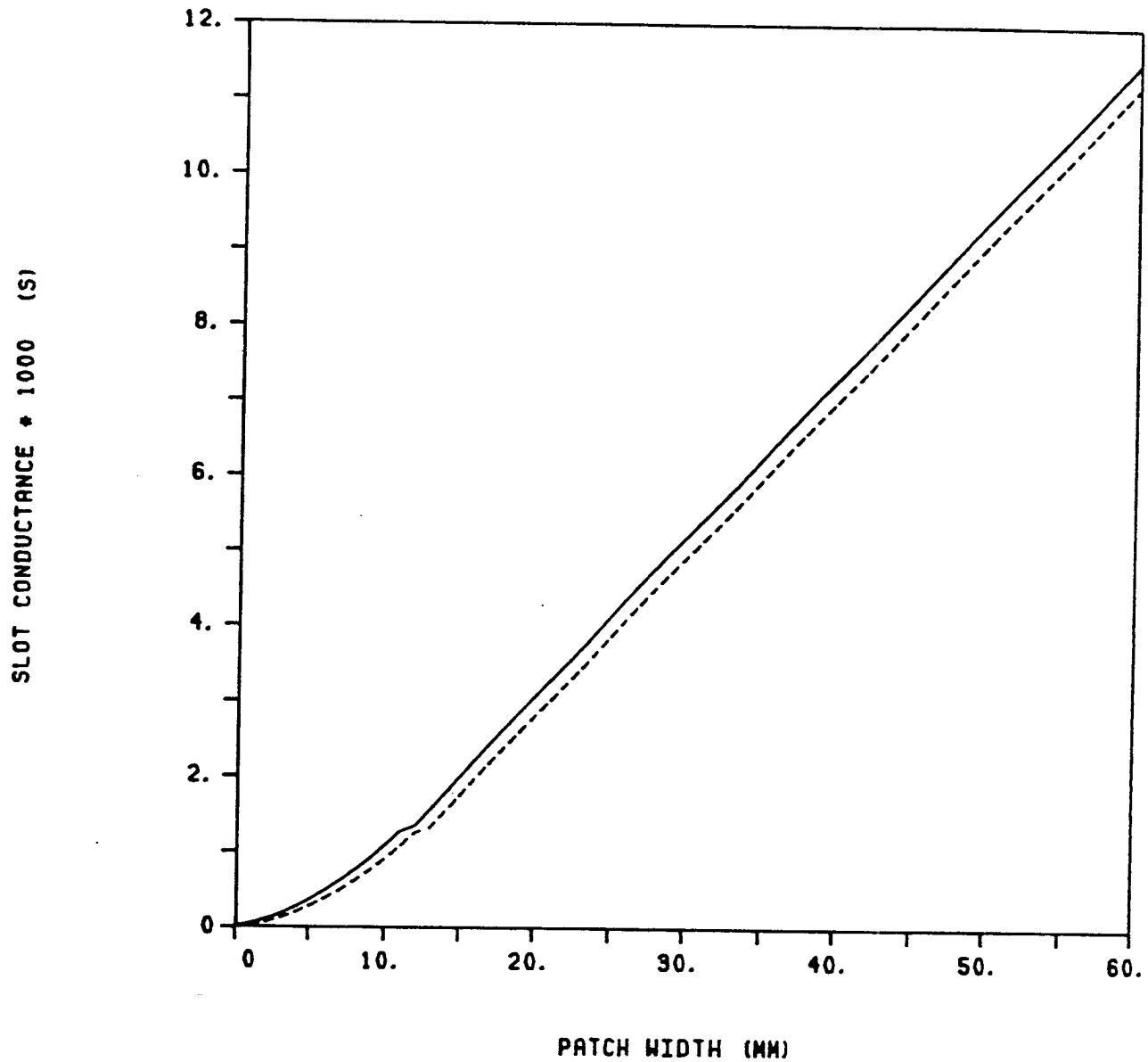

Figure 4.7 Slot conductance as a function of the patch width. f = 7.5 GHz and $\varepsilon_r = 2.2$. —— h = 1/32 in, - - - - h = 1/64 in

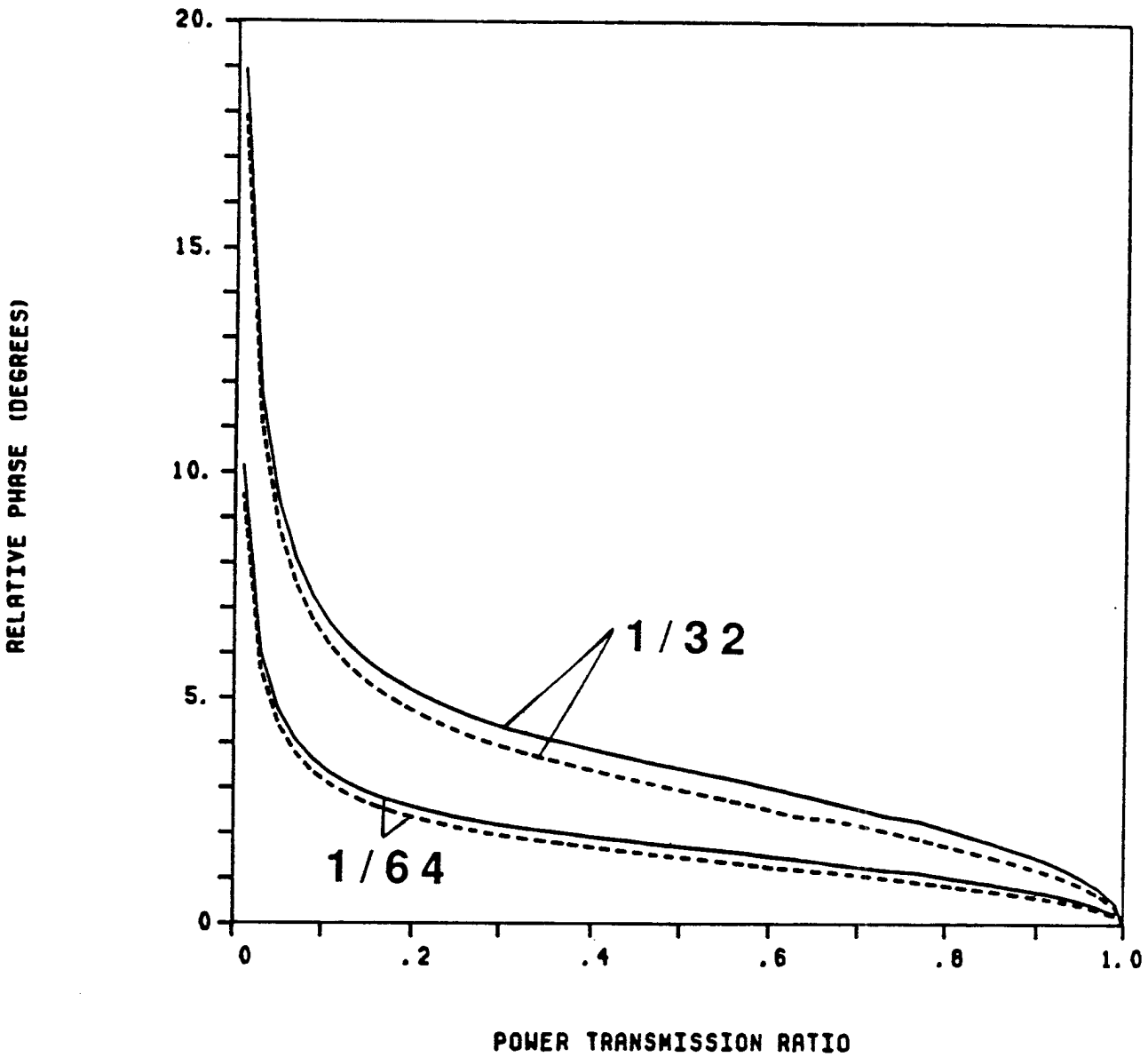

Figure 4.8 Relative phase of the transmitted signal as a function of the power transmission ratio for a rectangular patch. f = 7.5 GHz and ε_r = 2.2. —— $Z_1 = Z_2 = 50$ ohm, - - - - $Z_1 = Z_2 = 75$ ohm

5. BANDWIDTH CHARACTERISTICS

5.1 Preliminaries

In this section the frequency behaviour of a two-port rectangular microstrip antenna element is studied. It is assumed that the characteristic impedance levels of the transmission lines as well as the slot conductances do not change over the narrow frequency band of interest. Thus, only the impact of the different transmission lines is simulated.

The transfer scattering matrix formulation is used to calculate the frequency characteristics of the two-port network. The matrix is defined in the Appendix together with explicit matrix elements for a lossless transmission line and a shunt element.

The voltage across the left radiating slot in Figure 2.2 is

$$V_{SL} = \left[\cos\left(\frac{f}{f_0}\beta x_1\right) + j\frac{Y_R - Y_1}{Y_0}\sin\left(\frac{f}{f_0}\beta x_1\right)\right] V_1^+ + \left[\cos\left(\frac{f}{f_0}\beta x_1\right) + j\frac{Y_R + Y_1}{Y_0}\sin\left(\frac{f}{f_0}\beta x_1\right)\right] V_1^- \tag{5.1}$$

where V_1^+ and V_1^- are the incoming and the reflected voltages, respectively on the input transmission line. The actual frequency is f

while f_0 is the center frequency and Y_R is the equivalent input admittance at the input port seen to the right.

Similarly, the voltage across the output line is expressed as

$$V_2 = \left[\cos\frac{f}{f_0}\beta\left(x_2 - x_1\right) + j\frac{Y_L - Y_1}{Y_0}\sin\frac{f}{f_0}\beta\left(x_2 - x_1\right)\right]V_1^+ + \\ + \left[\cos\frac{f}{f_0}\beta\left(x_2 - x_1\right) + j\frac{Y_L + Y_1}{Y_0}\sin\frac{f}{f_0}\beta\left(x_2 - x_1\right)\right]V_1^- \tag{5.2}$$

where Y_L is the equivalent input admittance at the input port seen to the left.

Finally, the voltage across the right slot is

$$V_{SR} = [\cos\frac{f}{f_0}\beta\left(1 - x_1\right) - \frac{Y_2\left(Y_L - Y_1\right)}{Y_0^2}\sin\frac{f}{f_0}\beta\left(1 - x_2\right)\sin\frac{f}{f_0}\beta\left(x_2 - x_1\right) + \\ + j\left\{\frac{Y_2}{Y_0}\sin\frac{f}{f_0}\beta\left(1 - x_1\right)\cos\frac{f}{f_0}\beta\left(x_2 - x_1\right) + \frac{Y_L - Y_1}{Y_0}\sin\frac{f}{f_0}\beta\left(1 - x_1\right)\right\}]\,V_1^+ + \\ + [\cos\frac{f}{f_0}\beta\left(1 - x_1\right) - \frac{Y_2\left(Y_L + Y_1\right)}{Y_0^2}\sin\frac{f}{f_0}\beta\left(1 - x_2\right)\sin\frac{f}{f_0}\beta\left(x_2 - x_1\right) + \\ + j\left\{\frac{Y_2}{Y_0}\sin\frac{f}{f_0}\beta\left(1 - x_1\right)\cos\frac{f}{f_0}\beta\left(x_2 - x_1\right) + \frac{Y_L - Y_1}{Y_0}\sin\frac{f}{f_0}\beta\left(1 - x_1\right)\right\}]\,V_1^- \tag{5.3}$$

5.2 Constant patch width

An important parameter of an antenna element is the input voltage standing wave ratio as a function of the frequency. The bandwidth defined as the frequency range where the standing wave ratio is less than two is plotted in Figure 5.1 as a function of the power transmission ratio. The slot radiation conductance is constant and it is set to 1 mS. The characteristic impedance levels of the input and output lines are 50 ohm. The patch impedance level is 20 ohm. Two cases are displayed corresponding to the two possible locations of the output port relative to the input port location as discussed in section 4.1. The bandwidth increases with increased loading which is equivalent to more power being transmitted. The results for the two locations of the output port are almost identicial. The maximum bandwidth is about 20% for this particular set of parameters. The bandwidth for the unloaded patch of the same size is 1.8%.

Another parameter of interest is the phase variation of the slot voltages and of the output voltage across the frequency band. This limits the useful bandwidth from a sidelobe level and from a beam squint point of view. The phase variation across a 2% bandwidth is shown in Figure 5.2 as a function of the power transmission ratio. The phase variation across a fixed bandwith decreases as the loading increases. The case that is plotted corresponds to the output port located close to the input port. However, the results for the two possible output port locations are almost the same.

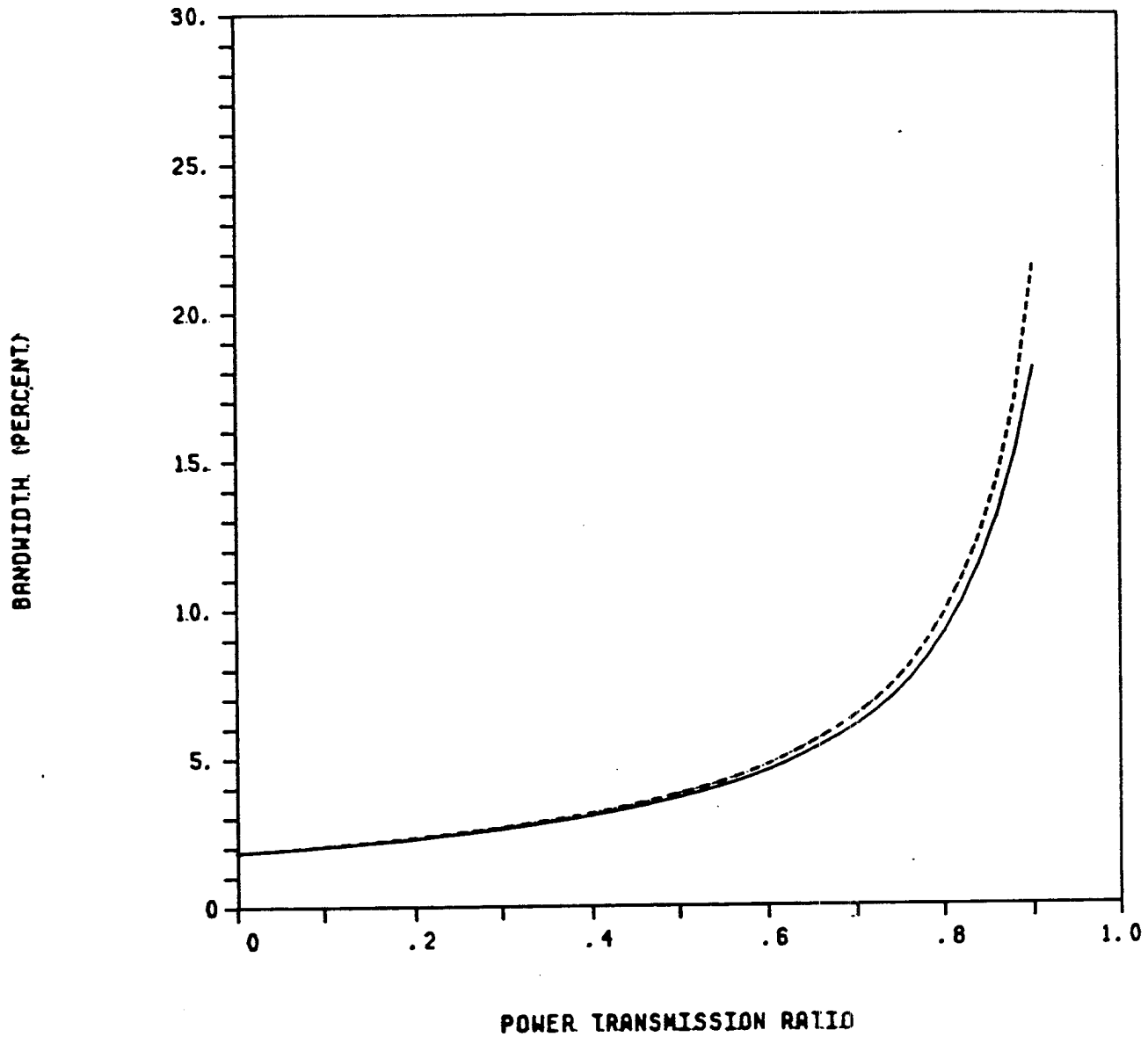

Figure 5.1 Calculated standing wave ratio bandwidth of a rectangular patch as a function of the power transmission ratio. Z_0 = 20 ohm, Z_1 = 50 ohm, Z_2 = 50 ohm, G = 1 mS and VSWR < 2. — = case1, - - - - = case 2

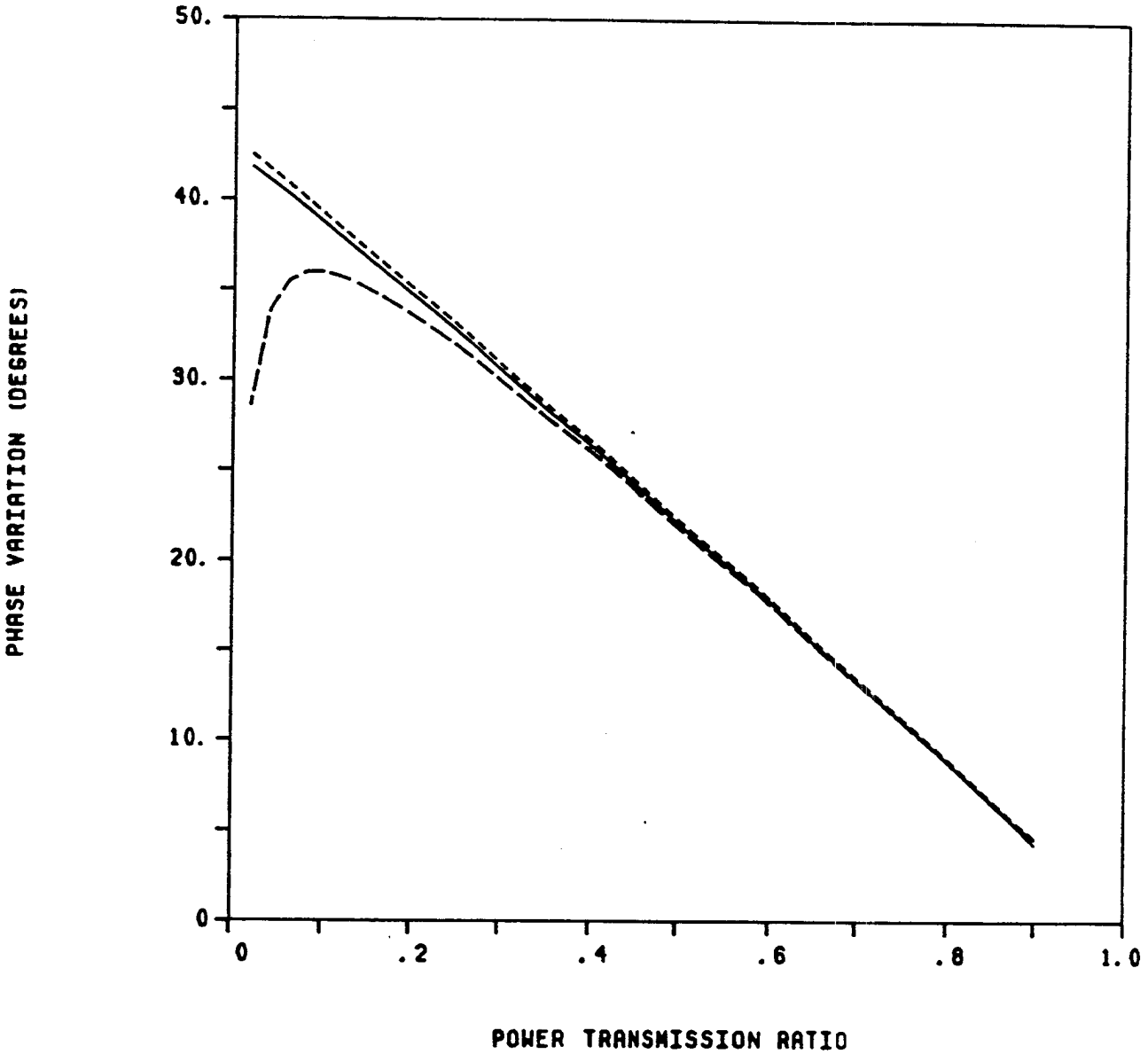

Figure 5.2 Computed phase variation across a 2% bandwidth of a rectangular patch as a function of the power transmission ratio. Z_0 = 20 ohm, Z_1 = 50 ohm, Z_2 = 50 ohm and G = 1 mS. —— = V_{SL}, - - - - = V_{SR}, _ _ _ _ = V_2

5.3 Optimum patch width

The phase difference between the radiating slot voltages is not necessarily 180 degrees for a patch of arbitrarily width. Therefore, the width is adjusted to obtain this requirement as discussed in Section 4.2. The voltage standing wave ratio bandwidth is plotted in Figure 5.3 as a function of the power transmission ratio for an optimum patch width. The bandwidth is defined as the frequency range where the standing wave ratio is less than two. Two substrate thicknesses are considered. As expected a doubling of the substrate thickness gives a doubling of the bandwidth. The bandwidth increases with increased power transmission ratio which is eqivalent to increased loading of the patch resonator. For a 80% power transmission ratio the bandwidth is 8.3% and 4.1% for a thickness of 1/32 in and 1/64 in, respectively. These values drop to 6.8% and 3.3%, respectively when the impedance level of the input and output lines is increased to 75 ohm. The patch width is about 10 mm.

The one-port element case corresponds to no power being transmitted. The bandwidth of such an element is 3.3% and 1.5% as shown in Figure 5.3 for the two thicknesses discussed. However, these results are valid for a 53 mm wide element as found in Figure 4.6. The bandwidth for a one-port element that is 10 mm wide is 1.7% and 0.7% for a thickness of 1/32 in and 1/64 in, respectively. The location of the input port is given by expression 3.11 with the proper set of parameters.

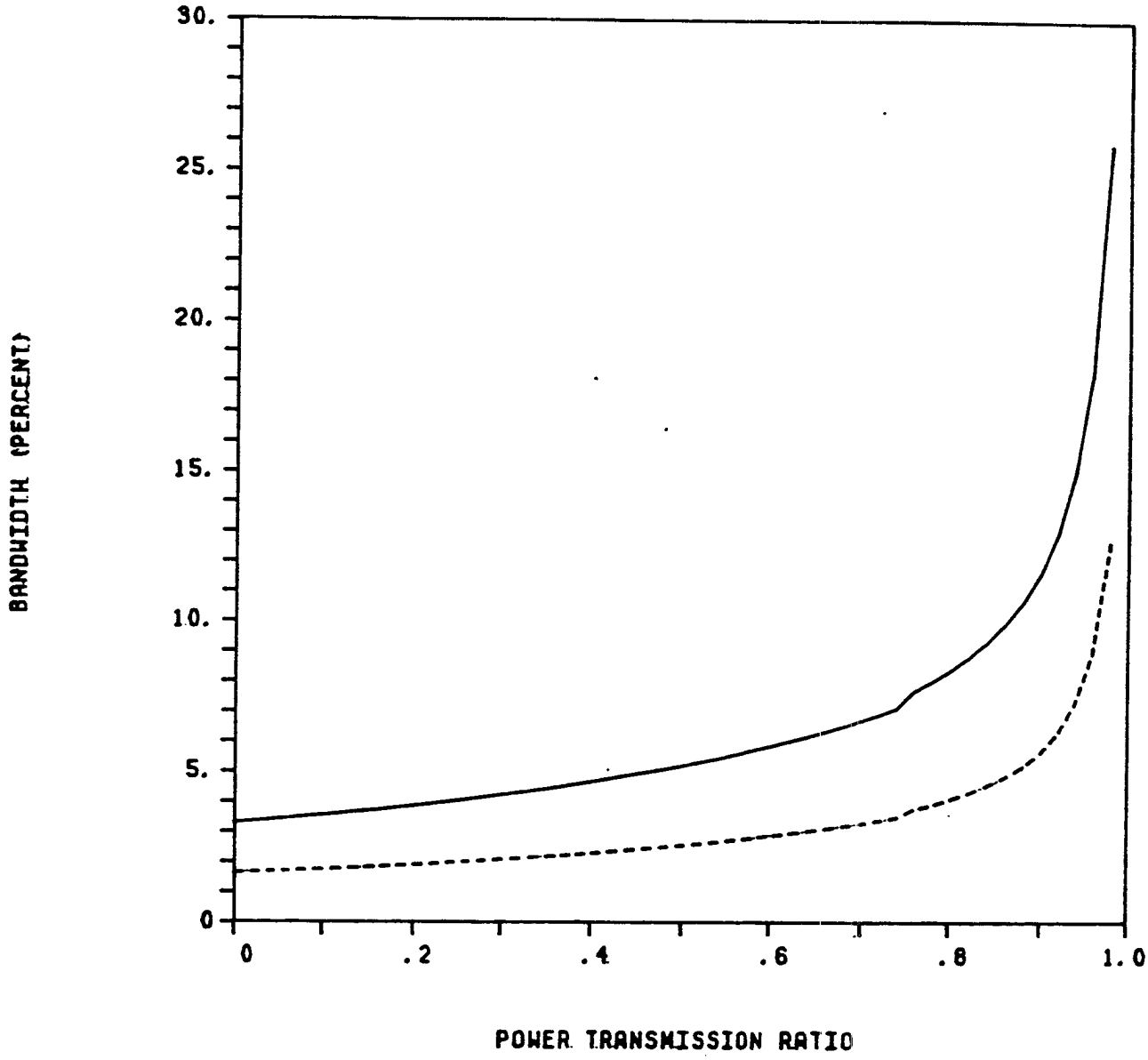

Figure 5.3 Computed standing wave ratio bandwidth of a rectangular patch as a function of the power transmission ratio. Z_1 = 50 ohm, Z_2 = 50 ohm, f_0 = 7.5 GHz, ε_r = 2.2 and VSWR < 2. —— h=1/32 in, - - - - h=1/64 in

The phase variations of the slot voltages and of the output voltage across a 2% bandwidth are shown in Figure 5.4 as a function of the power transmission ratio. Only two curves are plotted for each thickness since the variations in slot phases track each other very closely. This indicates that the phase difference between the slot voltages remains at 180 degrees across a relative large frequency band. The phase variation is less when the power transmission ratio is high.

An example of the relative phases as a function of the frequency is shown in Figure 5.5. The power transmission ratio is 80%. Two sets of curves are plotted corresponding to a 1/32 in and a 1/64 in substrate thickness, respectively. The resonant length of the patch is 180 degrees (14.00 mm and 13.76 mm) and the widths are 10.10 mm and 11.19 mm, respectively. The locations of the input ports are 3.26 mm and 3.20 mm, and the output ports are 3.75 mm and 3.68 mm, respectively from the left radiating slot. The phases change almost linearly with the frequency across the 10% band studied. Changing the impedance levels of the input and output lines from 50 ohm to 75 ohm slightly increases the slope of the phase curves.

The variation in radiated and transmitted power ratios as a function of the relative frequency is plotted in Figure 5.6 for a rectangular patch with the same set of parameters as above. The variation across the frequency band is larger for the thinner substrate case. Also a higher impedance level increases the variation. The power that is

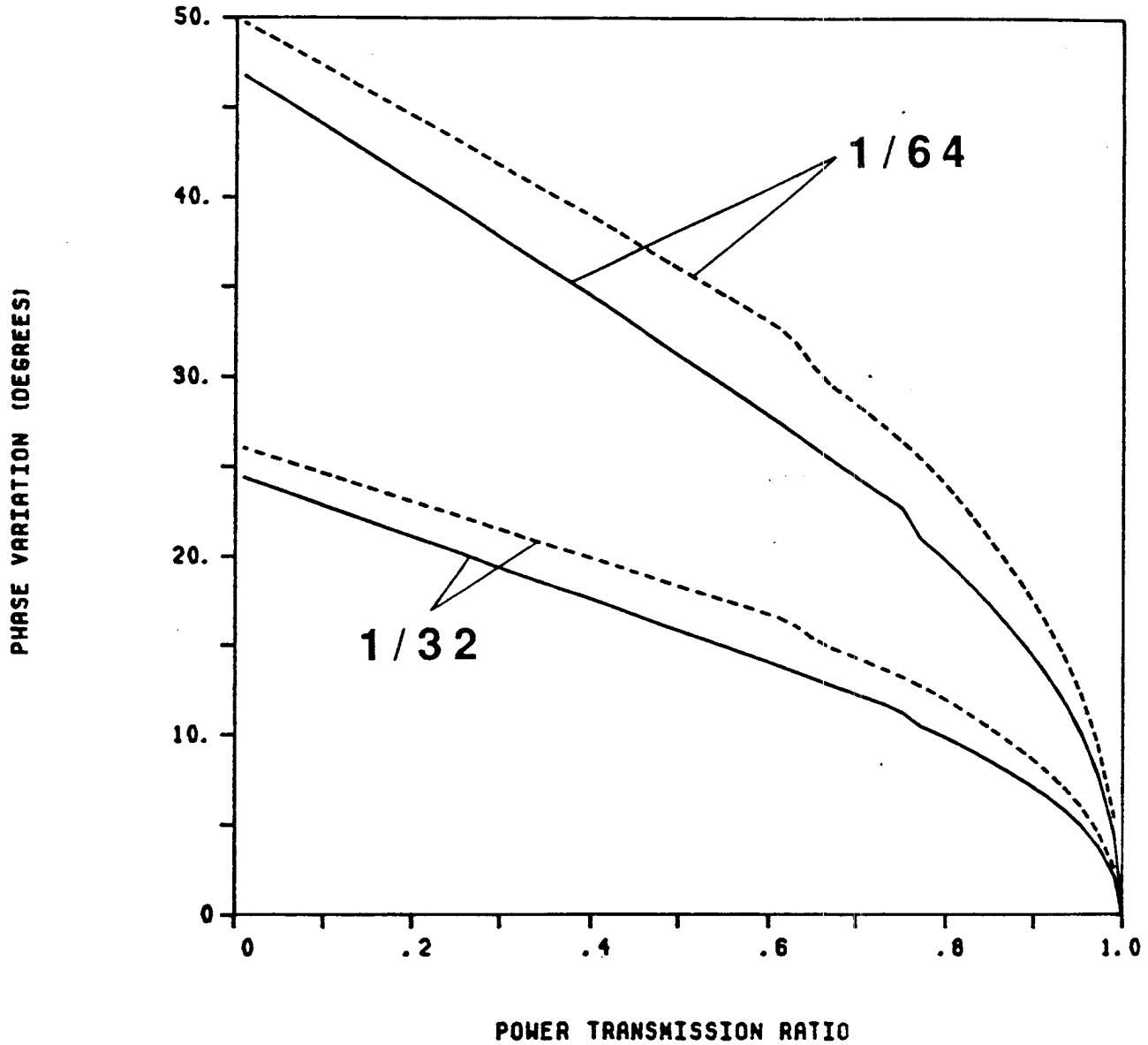

Figure 5.4 Computed phase variations of a rectangular patch as a function of the power transmission ratio across a 2% bandwidth. $f_0 = 7.5$ GHz and $\varepsilon_r = 2.2$. —— = $Z_1 = Z_2 = 50$ ohm, - - - - $Z_1 = Z_2 = 75$ ohm

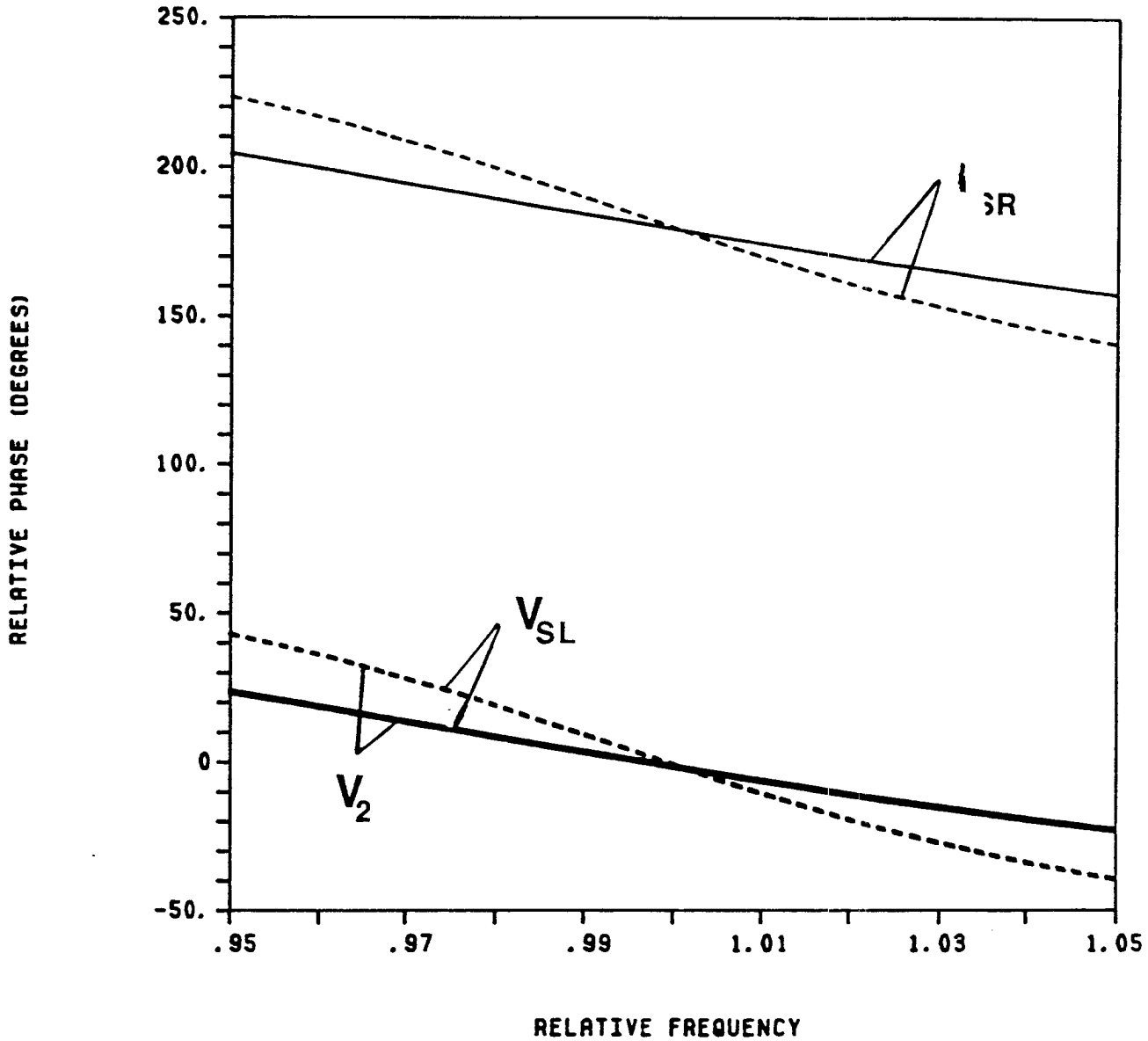

Figure 5.5 Computed relative phases of a rectangular patch as a function of the frequency. Z_1 = 50 ohm, Z_2 = 50 ohm, f_0 = 7.5 GHz, ε_r = 2.2. and T = 80%. —— h = 1/32 in , - - - - h = 1/64 in

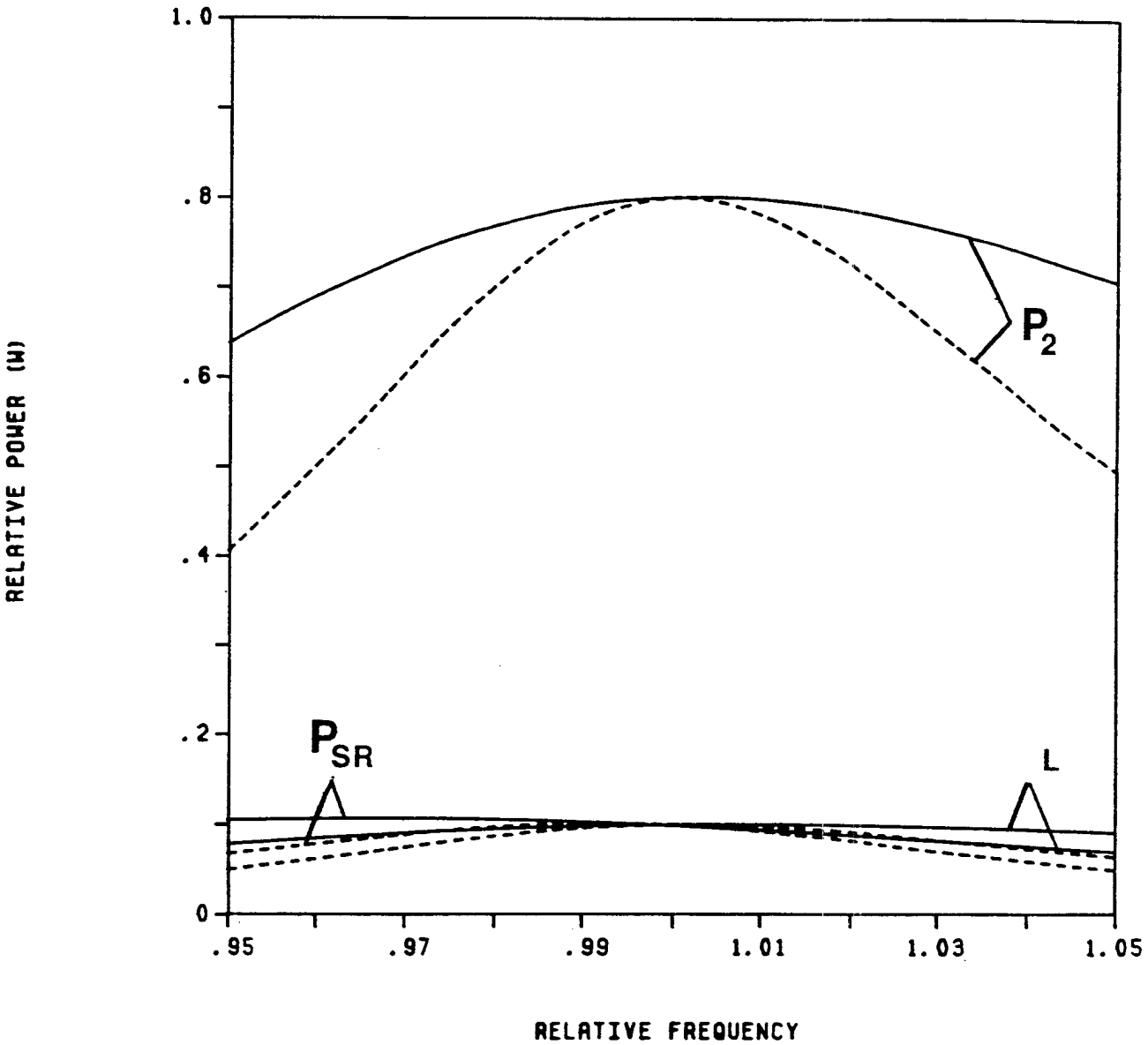

Figure 5.6 Computed power ratios of a rectangular patch as a function of the relative frequency. Z_1 = 50 ohm, Z_2 = 50 ohm, f_0 = 7.5 GHz, ε_r = 2.2 and T = 80%. —— h = 1/32 in, - - - - h = 1/64 in

neither transmitted nor radiated is reflected causing an increased standing wave ratio.

6. CONCLUSIONS

A two-port rectangular microstrip antenna element is described that has the potential to be very broadband. The increased bandwidth is achieved by loading the antenna which is equivalent to lowering the Q-factor of the resonator making the frequency variation less pronounced.

The two-port element is matched at the input port by properly selecting the locations of the input and output ports. At the same time the radiated power ratio is controlled. To make sure the phase difference between the radiating slot voltages is 180 degrees the width of the patch is adjusted as the power transmission ratio is altered.

The standing wave ratio bandwidth of the two-port radiating element is greater than 20% for practical values of substrate parameters and high power transmission ratios. This feature of the two-port element is particularly applicable in series-fed array applications. In such designs, the radiated power at each element is a small fraction of the total input power. Most of the input power into each element is thus transmitted to the next radiator thereby

considerably increasing the bandwidth of the single patch. The bandwidth of a corresponding one-port element is of the order of 1%.

The transmission phase of a two-port antenna element changes as the power transmission ratio is altered. However, the variation is less when the power transmission ratio is high which is the most likely state of operation in a series-fed array application. The impact of this is that the length of the interconnecting lines in a series-fed array have to be adjusted accordingly to compensate for the phase differences.

Design equations for the two-port rectangular microstrip antenna element are given that are based on the transmission-line model. These equations are simple to solve. The results can therefore be used as starting values in a more complete and time-consuming optimization procedure.

REFERENCES

1. A. G. Derneryd, "Linearly polarized microstrip antennas", IEEE Trans. Antennas Propagat., vol. AP-24, pp. 846-850, Nov. 1976

2. T. Metzler, "Microstrip series arrays", Proc. Workshop on Printed Circuit Antenna Tech., New Mexico State University, Las Cruses, pp. 20.1-20.16, Oct. 1979

3. W. Menzel, "A 40 GHz microstrip array antenna", Proc. IEEE MTT-S Int. Symp., pp. 225-226, May 1980

4. F. Lalezani and C. D. Massey, "Mm-wave microstrip antennas", Microwave J., vol. 30, pp. 87-96, April 1987

5. M. Danielsen and R. Jorgensen, "Frequency scanning microstrip antennas", IEEE Trans. Antennas Propagat., vol. AP-27, pp. 146-150, March 1981

6. M. Jayachandran and S. C. Gupta, "Frequency scanning microstrip antenna (S-band)", Proc. IRSI83, India, pp. 175-180, 1983

7. K. C. Gupta, R. Garg and R. Chadha, "Computer-aided design of microstrip circuits", Artech House, Dedham, MA, p. 61, 1981

8. J. R. James, P. S. Hall and C. Wood, "Microstrip antenna. Theory and design", Peter Peregrinus Ltd, Stevenage, UK, p. 88, 1981

9. A. Benalla and K. C. Gupta, "Two dimensional analysis of one-port and two-port rectangular microstrip antennas", Report No. 85, Electromagnetics Laboratory, Univ. of Colorado, Boulder, CO, May 1986

10. IMSL Library, Subroutine ZSPOW, Edition 9, June 1982

11. K. C. Gupta, "Two-port transmission characteristics of rectangular microstrip patch radiators", IEEE AP-S Int. Sym. Digest, pp. 71-73, June 1985

APPENDIX

THE TRANSFER SCATTERING MATRIX

The transfer scattering matrix is defined as

$$\begin{pmatrix} b_1 \\ a_1 \end{pmatrix} = \begin{pmatrix} T_{11} & T_{12} \\ T_{21} & T_{22} \end{pmatrix} \begin{pmatrix} a_2 \\ b_2 \end{pmatrix} \tag{A.1}$$

where the incoming and outgoing waves are defined in Figure A.1.

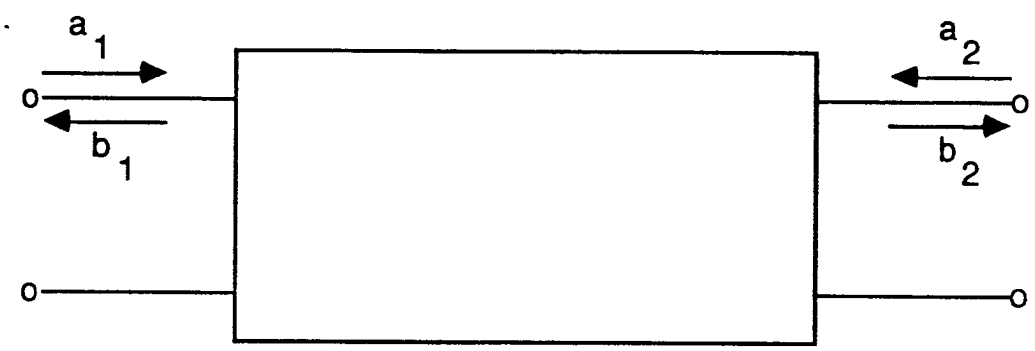

Figure A.1 Transfer scattering matrix references

The advantage of the transfer scattering matrix formulation is that the overall matrix of a cascaded network is obtained by multiplying the individual transfer scattering matrices.

The transfer scattering matrix of a lossless transmission line of length x as shown in Figure A.2 is

$$(T) = \begin{pmatrix} e^{-j\beta x} & 0 \\ 0 & e^{j\beta x} \end{pmatrix} \tag{A.2}$$

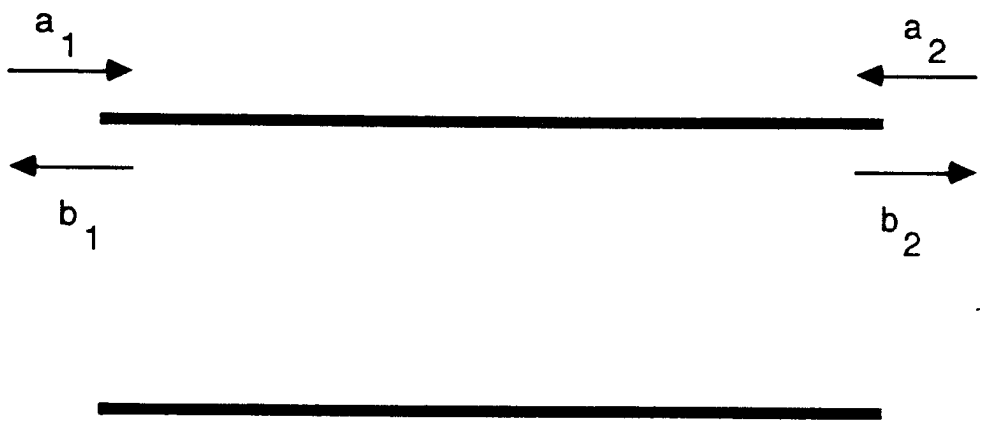

Figure A.2 Transmission line with no losses

Finally, the transfer scattering matrix of a shunt element between two transmission lines of unequal admittance levels as given in Figure A.3 is

$$(T) = \frac{1}{2Y_1}\begin{pmatrix} Y_1 + Y_2 - Y & Y_1 - Y_2 - Y \\ Y_1 - Y_2 + Y & Y_1 + Y_2 + Y \end{pmatrix} \qquad (A.3)$$

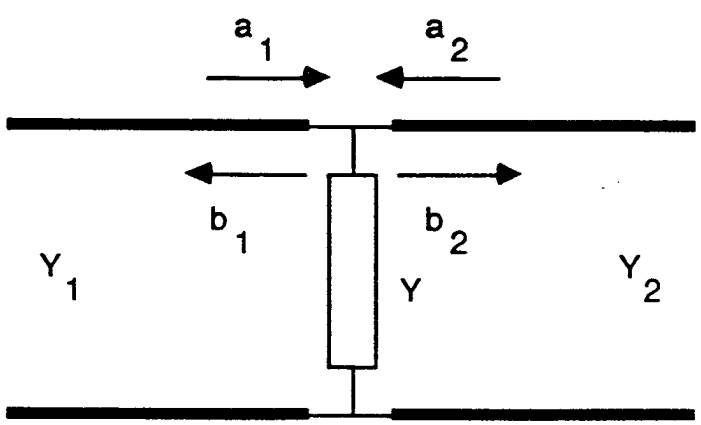

Figure A.3 Shunt element between transmission lines of unequal admittance levels